

**DESIGN OF A SWIMMING SMALL
SOFT ROBOT FOR
UNDERWATER APPLICATIONS**

CHAVEZ CHIN ZHEE MING

UNIVERSITI TUNKU ABDUL RAHMAN

**DESIGN OF A SWIMMING SMALL SOFT ROBOT FOR
UNDERWATER APPLICATIONS**

CHAVEZ CHIN ZHEE MING


**A project report submitted in partial fulfilment of the
requirements for the award of Bachelor of Mechatronics
Engineering with Honours**

**Lee Kong Chian Faculty of Engineering and Science
Universiti Tunku Abdul Rahman**

October 2024

DECLARATION

I hereby declare that this project report is based on my original work except for citations and quotations which have been duly acknowledged. I also declare that it has not been previously and concurrently submitted for any other degree or award at UTAR or other institutions.

Signature :  _____

Name : CHAVEZ CHIN ZHEE MING

ID No. : 2004767

Date : 1 October 2024

APPROVAL FOR SUBMISSION

I certify that this project report entitled “**DESIGN OF A SWIMMING SMALL SOFT ROBOT FOR UNDERWATER APPLICATIONS**” was prepared by **CHAVEZ CHIN ZHEE MING** has met the required standard for submission in partial fulfilment of the requirements for the award of Bachelor of Mechatronics Engineering with Honours at Universiti Tunku Abdul Rahman.

Approved by,

Signature

:



Supervisor

:

Dr Low Jen Hahn

Date

:

1 October 2024

The copyright of this report belongs to the author under the terms of the copyright Act 1987 as qualified by Intellectual Property Policy of Universiti Tunku Abdul Rahman. Due acknowledgement shall always be made of the use of any material contained in, or derived from, this report.

© 2024, CHAVEZ CHIN ZHEE MING. All right reserved.

ACKNOWLEDGEMENTS

I would like to extend my deepest appreciation to all those who contributed to the successful completion of this Final Year Project. First and foremost, I am profoundly grateful to my research supervisor, Dr. Low Jen Hahn, for his unwavering guidance, insightful advice, and immense patience throughout the development of this research. His dedication to academic excellence and encouragement pushed me to strive for the highest standards, motivating me to give my utmost to meet his expectations. I would also like to sincerely thank Dr. Tan Li Fan for his invaluable and constructive feedback, which greatly improved both my presentation and final report. My gratitude also goes to Dr. Chee Pei Song for his innovative suggestions and ideas regarding the prototype design, and to Dr. Danny for his expert guidance in the realms of electrical and electronics engineering. Furthermore, I am grateful to Dr. See Yuen Chark for his strategic advice, which helped shape my approach to the FYP Poster Competition, and to Dr. Hau Lee Cheun for his support and informative advice as the FYP course coordinator.

In addition to the academic support I received, I am deeply thankful to my parents, whose unwavering love and practical assistance, especially in providing transportation to campus that enabled me to maximize my productivity without the added strain of commuting via public transport. I am also grateful to my fellow peers Teck Yuan and Wayne, who, as fellow students under Dr. Low's supervision, offered continuous encouragement and support when I faced challenges, particularly during the hectic final trimester. I am indebted to Zhi Xuan, Ying Hang, and Jun Han for their assistance with the experimental setups, and to Xin Yan and Kevin for their help in 3D-printing molds essential to the fabrication of my prototype. Lastly, my heartfelt thanks go to Cherrie, whose emotional support has been a constant source of strength throughout this journey, helping me stay focused and grounded even during the most stressful moments.

ABSTRACT

Traditional rigid robots, while effective in many applications, present significant challenges in environments involving human interaction or delicate objects due to their inflexible structure, which can cause damage or accidents upon collision. Additionally, rigid robots require precise control mechanisms, limiting their adaptability to unpredictable conditions. In contrast, soft robots offer a safer, more versatile alternative. Their inherent elasticity reduces the risk of injury or damage during collisions and allows them to adapt to complex environments more effectively. This study investigates the application of biological locomotion mechanisms in a soft robot designed for underwater swimming. By utilizing flexible materials like Ecoflex, PVC sheets, and plastic films, the study successfully developed a soft robot capable of actuating in water. Key findings indicate that the robot was able to swim in a straight path, with optimal performance observed at an actuation frequency of 1.33 Hz and a pump voltage of 11 V. A second prototype validated directional control, allowing the robot to turn and manoeuvre precisely. This directional control, along with linear swimming, was incorporated into a swimming algorithm controlled by three push buttons. These advances contribute to the potential for soft robots in applications such as search-and-rescue operations, underwater exploration, and water quality monitoring.

TABLE OF CONTENTS

DECLARATION		i
APPROVAL FOR SUBMISSION		ii
ACKNOWLEDGEMENTS		iv
ABSTRACT		v
TABLE OF CONTENTS		vi
LIST OF TABLES		ix
LIST OF FIGURES		x
LIST OF APPENDICES		xiii
CHAPTER		
1	INTRODUCTION	1
1.1	General Introduction	1
1.2	Importance of the Study	1
1.3	Problem Statement	2
1.4	Aim and Objectives	2
1.5	Scope and Limitation of the Study	3
1.6	Contribution of the Study	3
1.7	Outline of the Report	4
2	LITERATURE REVIEW	5
2.1	Introduction	5
2.2	Materials	5
2.2.1	Silicone Elastomer	5
2.2.2	Hydrogel	7
2.3	Types of Actuation	8
2.3.1	Electrically Responsive	8
2.3.2	Magnetically Responsive	9
2.3.3	Thermally Responsive	10
2.3.4	Photo Responsive	13
2.3.5	Pressure Driven	14

2.4	Soft Actuator Structure	17
	2.4.1 Ribbed Structures	17
	2.4.2 Cylindrical Structures	18
	2.4.3 Pleated Structures	19
2.5	Locomotion Inspiration	20
	2.5.1 Eel-Inspired	20
	2.5.2 Frog-Inspired	22
	2.5.3 Butterfly-Inspired	23
2.6	Hardware	23
	2.6.1 Arduino UNO	24
	2.6.2 ESP32	24
	2.6.3 Micro Vacuum Air Pump and Micro Solenoid Valve	24
2.7	Summary	25
3	METHODOLOGY AND WORK PLAN	27
3.1	Introduction	27
3.2	Soft Robot Design	27
	3.2.1 Materials	29
	3.2.2 Structure	30
	3.2.3 Actuation	31
	3.2.4 Control and Electronics	32
3.3	Fabrication	33
	3.3.1 Preparation of Mold	35
	3.3.2 Ecoflex Casting and Assembly Process	35
	3.3.3 Constructing the Electrical and Pneumatic Circuit	36
3.4	Experiment Procedures	37
3.5	Gantt Chart	39
3.6	Summary	40
4	RESULTS AND DISCUSSION	41
4.1	Introduction	41
4.2	Simulation	41
4.3	Characterisation	43
4.4	Swimming Performance	45

4.4.1	Linear Swimming Motion	45
4.4.2	Parameters for Optimum Swimming Performance in Linear Path	46
4.4.3	Directional Control	47
4.4.4	Swimming Algorithm	48
4.5	Biomechanics of Butterfly Stroke	48
4.6	Summary	51
5	CONCLUSIONS AND RECOMMENDATIONS	52
5.1	Conclusions	52
5.2	Recommendations for Future Work	52
	REFERENCES	54
	APPENDICES	58

LIST OF TABLES

Table 3.1:	Comparison of Young's modulus of different materials.	29
Table 3.2:	Gantt Chart for FYP 1.	39
Table 3.3:	Gantt Chart for FYP 2.	40

LIST OF FIGURES

Figure 2.1:	Chemical structure of silicone elastomer.	6
Figure 2.2:	Ecoflex.	7
Figure 2.3:	Chemical structure of hydrogel.	7
Figure 2.4:	Deformation of DEAs. Reprinted with permission from copyright 2017 Springer Nature.	8
Figure 2.5:	Types of DEAs. (a) Layer by layer stacked actuator; (b) folded actuator; (c) helical actuator. Reprinted with permission from copyright 2017 Springer Nature.	9
Figure 2.6:	Shapes of deformation for the magnetically responsive actuator. Reprinted with permission from copyright 2016 IEEE.	10
Figure 2.7:	State of SMP under different temperatures. Reprinted with permission from copyright 2023 Springer Nature.	11
Figure 2.8:	Deformation of LCE at low and high temperatures. Reprinted with permission from copyright 2017 Springer Nature.	12
Figure 2.9:	Deformation of NIR light-driven actuator. Reprinted with permission from copyright 2023 IEEE.	14
Figure 2.10:	Unpressurised state and pressurised state of soft pneumatic actuator. Reprinted with permission from copyright 2016 IEEE.	16
Figure 2.11:	Pressurisation of a soft hydraulic actuator. Reprinted with permission from copyright 2016 IEEE.	17
Figure 2.12:	Concept of a ribbed segment. (a) Before the air chambers are pressurized (b) After the air chambers are pressurized. Reprinted with permission from copyright 2012 John Wiley and Sons.	18
Figure 2.13:	Concept of cylindrical segment. (a) Before the channels are pressurized (b) After the channels are pressurized. Reprinted with permission from copyright 2012 John Wiley and Sons.	19
Figure 2.14:	Concept of a pleated segment. (a) The cross-sectional area of the hollow channels before being pressurized (b) The cross-sectional area of hollow channels after being	

pressurized. Reprinted with permission from copyright 2012 John Wiley and Sons.	20
Figure 2.15: Eel-inspired design. Reprinted with permission from copyright 2017 Mary Ann Liebert, Inc.	21
Figure 2.16: Frog-inspired design. Reprinted with permission from copyright 2020 Mary Ann Liebert, Inc.	22
Figure 2.17: Micro vacuum air pump with solenoid.	25
Figure 3.1: 3D CAD drawing of the soft robot.	28
Figure 3.2: Pneumatic channels in one soft bending actuator.	28
Figure 3.3: Part A and Part B of Ecoflex.	30
Figure 3.4: Polyester sheets.	30
Figure 3.5: 12 V DC micro vacuum air pump.	31
Figure 3.6: Micro solenoid valves.	31
Figure 3.7: Arduino UNO board.	32
Figure 3.8: 4-channel relay.	33
Figure 3.9: Pneumatic schematic diagram.	33
Figure 3.10: Flowchart of fabrication plan.	34
Figure 3.11: First prototype with single actuation body.	34
Figure 3.12: Second prototype with two actuation bodies.	35
Figure 3.13: Mold for (a) side layers and (b) middle layer.	35
Figure 3.14: Assembly process.	36
Figure 3.15: Electrical and pneumatic circuit.	37
Figure 3.16: Soft actuator floating on water surface from (a) side view and (b) isometric view.	38
Figure 3.17: Setup for first prototype swimming straight.	38
Figure 3.18: Setup for second prototype turning right.	39

Figure 4.1:	Deformation of the soft bending actuator under pressure (a) $P = 1$ MPa (b) $P = 2$ MPa (c) $P = 3$ MPa (d) $P = 4$ MPa.	43
Figure 4.2:	Deformation of the soft actuator.	44
Figure 4.3:	Graph of bending angle vs pump voltage.	44
Figure 4.4:	Soft robot position at $t = 0$ s.	45
Figure 4.5:	Soft robot position at $t = 10$ s.	45
Figure 4.6:	Pressure level in upper and lower pneumatic chamber at (a) 5 Hz and (b) 1 Hz.	46
Figure 4.7:	Time taken to swim in linear path for different actuation frequencies with optimum actuation frequency circled.	47
Figure 4.8:	Time taken to swim in linear path for different pump voltages with optimum pump voltages circled.	47
Figure 4.9:	Robot (a) before turning right and (b) after turning right.	48
Figure 4.10:	Butterfly stroke swimming style.	49

LIST OF APPENDICES

Appendix A: Coding for Swimming Algorithm	58
Appendix B: Supporting attachment for FYP Competition Shortlisting	61
Appendix C: Supporting attachment for FYP Competition Bronze Award	62
Appendix D: Open Access to Image Rights	63

CHAPTER 1

INTRODUCTION

1.1 General Introduction

Soft robotics is a growing field that involves applying the locomotion mechanisms of animals in nature to achieve smooth and complex motion. Animals are classified as soft bodies due to their soft tendon, flesh, and muscles. Some sources of inspiration for the locomotion mechanism of soft robots are earthworms, snakes, octopuses, eels, jellyfish, and the human hand. By applying locomotion mechanisms developed in nature over a long time onto robots, robots can move in complex environments. The term “soft robot” first emerged in the field referring to a mechanical gripper that utilizes soft, elastic materials at the interface with the object of interest (Tondu and Lopez, 2000). The term “soft robot” later refers to a robot with its structure entirely made up of elastic and deformable materials. These soft robots offer unique advantages in applications in constrained environments such as tight space manoeuvring and underwater exploration. By mimicking the locomotion and behaviour of aquatic creatures, swimming soft robots have great potential and reliability in transforming underwater robotics (Rus & Sitti, 2014).

1.2 Importance of the Study

Traditional rigid robots often have the problem of operating in unfamiliar environments, where they are generally hard-programmed to work in familiar environments. Besides, rigid robots also have the risk of causing harm and injuries to humans and other living creatures. However, this is hardly a challenge to soft robots as their ability to deform provides them with higher flexibility to adapt to different settings. Depending on the design, a soft robot can be programmed to produce both simple and complex movements. Soft robots are widely applied in the medical field due to their nonrigid mechanical structure and adaptivity to wearable medical devices. In underwater exploration, their ability to navigate complex underwater terrain, interact delicately with marine life, and execute tasks with precision makes them invaluable in fields such as marine biology, oceanography, underwater

archaeology, and environmental monitoring (Calisti et al., 2018). Nonetheless, despite recent developments, optimization of efficiency, manoeuvrability, and endurance of swimming soft robots remains a barrier on the path of advancement.

1.3 Problem Statement

Traditional rigid robots, while effective in controlled environments, face significant challenges when deployed in delicate ecosystems such as coral reefs and other marine habitats. The rigid structures of these robots can inadvertently cause damage to marine life and the surrounding environment. For example, the sharp edges and hard surfaces of rigid robots may accidentally harm coral reefs, disrupt fragile ecosystems, or injure marine organisms due to their lack of flexibility and adaptability (Smith & Jones, 2018). In response to these limitations, the emerging field of soft robotics offers a promising alternative. Soft robots, inspired by the natural movements and characteristics of organisms, possess inherent flexibility and compliance that enable them to navigate complex and dynamic environments with minimal impact. By leveraging soft materials and innovative design principles, soft robots can mitigate the risks associated with rigid robots and provide more sustainable solutions for underwater exploration and intervention tasks (Park et al., 2020).

In the underwater realm, the benefits of soft robotics become particularly pronounced. Soft robots excel in tasks such as underwater inspection, maintenance of underwater infrastructure, and marine research, where precision, manoeuvrability, and non-intrusiveness are paramount. Their ability to conform to irregular surfaces and interact gently with marine life makes them ideal for studying fragile ecosystems, conducting non-destructive sampling, and performing underwater interventions with minimal disturbance (Brown & Smith, 2019).

1.4 Aim and Objectives

This project aims to develop a small swimming soft robot to operate around the water surface. The objectives of this project are as shown below:

1. To review soft robots in terms of design, materials, and locomotion algorithm.
2. To design a soft robot using soft materials.
3. To develop an algorithm of robot swimming locomotion using suitable actuating mechanism.

1.5 Scope and Limitation of the Study

The direction of this study is to focus on the designation of a swimming soft robot that can be implemented in underwater exploration, surveillance, and intervention tasks. The actuation mechanism, soft robot structure design, and control circuit are the main focus of this research. However, there exist several hurdles that might affect the research outcome.

To achieve different ranges and speeds of motion, the actuating frequency and force should be experimented with, and the soft robot structure can be redesigned to different thicknesses, lengths, and so on. While the alteration of actuating mechanism can be achieved in a relatively easy manner, refabricating the robot can increase the cost of research due to the increased amount of elastic material used for structure fabrication. Besides, due to the requirement to interact with water, the control circuit should be located away from the robot and water for safety reasons. Therefore, a tubing connection in the form of pneumatic tubing for pneumatic actuation, or wire for heating shape memory alloy or polymer. Furthermore, as there is a size constraint in the aquarium used for the experiment, the soft robot is preferred to be small, yet there exists a minimum size limit.

1.6 Contribution of the Study

This study contributes to the field of soft robotics by exploring new materials, design principles, and control algorithms that enhance the performance, adaptability, and safety of soft robots in underwater applications. The development of a novel swimming soft robot showcases how bio-inspired designs and soft actuators can address the challenges of operating in complex, unstructured environments. One significant contribution is the robot's potential use in water quality monitoring, where its flexibility and gentle interaction

with delicate ecosystems can aid in gathering data without causing disruption. Additionally, the robot's adaptability makes it suitable for responding to environmental disasters, such as oil spills or marine habitat degradation, and performing essential tasks in confined or hazardous underwater areas. This research not only advances the design of soft robots but also highlights their growing relevance in environmental monitoring and disaster response.

1.7 Outline of the Report

The report is structured into five chapters, each addressing a specific aspect of the study. Chapter 1 introduces the project, offering a background on soft robotics, including its working principles, materials, and advantages. This chapter also presents the problem statement, research objectives, significance of the study, and its limitations.

Chapter 2 provides an in-depth literature review, exploring recent advancements in soft robotics, such as material innovations, actuation methods, actuator structures, and various locomotion strategies.

Chapter 3 outlines the study's methodology, depicted through a detailed flowchart, and lists the necessary simulation software, materials, and equipment. It thoroughly explains the design process, fabrication techniques, characterisation methods, and the testing procedures for evaluating the robot's swimming performance.

Chapter 4 presents the experimental results, highlighting the robot's ability to float, swim in a straight line, and the identification of optimal actuation parameters. Additionally, it validates the directional control capabilities of the robot.

Chapter 5 concludes the report by summarising the key findings and offering recommendations for future research directions to further enhance soft robotics technology.

CHAPTER 2

LITERATURE REVIEW

2.1 Introduction

Soft robotics is a rapidly advancing field that draws inspiration from biological systems, utilizing soft materials and various types of actuators for design, fabrication, and control. Soft robots are designed to perform tasks that are challenging or impossible for traditional rigid robots, such as manipulating delicate items and adapting to unstructured environments. They find applications across diverse fields including healthcare, manufacturing, research, and rescue missions.

Soft robots exhibit flexibility and are capable of performing tasks that are typically challenging for rigid robots. Their design primarily incorporates soft and flexible materials that can deform under specific conditions, such as silicone elastomers, polymers, or hydrogels. Actuators play a crucial role in controlling the movement of soft robots, with options including hydraulic, pneumatic, or shape-memory alloy actuators. Additionally, soft robots rely on control systems to manage their movements and responses, often employing computer-based or feedback loop control systems.

2.2 Materials

Soft robotics relies heavily on the selection of appropriate materials to achieve desired mechanical properties, flexibility, and biocompatibility. Various materials have been explored for soft robot fabrication, with silicone elastomers, and hydrogels being among the most prominent.

2.2.1 Silicone Elastomer

Silicone elastomer is a flexible and stretchable material composed of silicone and various other molecules, including carbon, hydrogen, and oxygen. Known for its durability, it exhibits high resistance to both chemical and temperature extremes, withstanding temperatures ranging from approximately -50°C to 350°C . The structure of silicone elastomer consists of a siloxane backbone with organic moieties bound to the silicone, as illustrated in Figure 2.1.

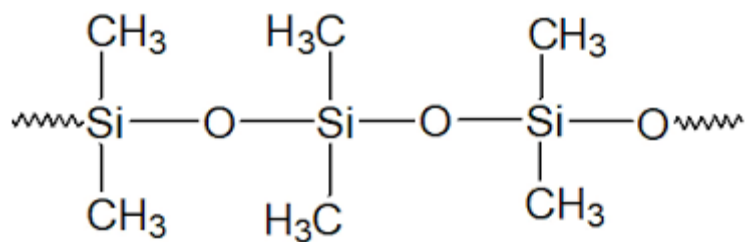


Figure 2.1: Chemical structure of silicone elastomer.

2.2.1.1 Polydimethylsiloxane (PDMS)

Polydimethylsiloxane (PDMS) falls under the umbrella of silicone elastomers and is extensively utilized in microfluidic applications for creating micro-devices, owing to its exceptional attributes such as flexibility, cost-effectiveness, and user-friendliness. The typical formulations of PDMS like Sylgard 184, the Young's modulus is usually around 0.5 to 3 MPa. While PDMS can be integrated into the design of soft robots due to its elasticity, it does have a downside where its mechanical properties are limited. To address this challenge, strategies such as blending pure PDMS with other polymers or incorporating particles have been employed to bolster its strength (Ariati et al., 2021).

2.2.1.2 Ecoflex

Ecoflex stands out as a widely used silicone elastomer, particularly favored for fabrication purposes. Produced by Smooth-On, Inc., it serves various applications including mold-making, casting, and artistic endeavors, as well as in industrial contexts such as the development of soft robots. The Young's modulus of Ecoflex, a widely used silicone elastomer, typically ranges from 50 kPa to 250 kPa depending on the specific grade and formulation. The Young's modulus of Ecoflex 00-30 and 00-50 are generally 125 kPa and 200 kPa. Referring to Figure 2.2, Ecoflex is typically mixed in a 1A : 1B ratio by weight and cured at room temperature. Renowned for its soft and stretchy properties, it is highly regarded as an excellent material choice for constructing soft robots.



Figure 2.2: Ecoflex.

2.2.2 Hydrogel

Hydrogels consist primarily of a network structure comprising water and hydrophilic polymer chains (Lee et al., 2018; Yang and Suo, 2018; Yuk et al., 2019). This polymer network can be tailored, enabling the hydrogel to withstand strains of up to 1000% (Sun et al., 2012). With a significant water volume fraction, hydrogels typically exhibit an elastic modulus ranging from 1 to 100 kPa. They find application in soft robotics due to their unique properties. The presence of dissolved ions in water imparts a conductivity of 10 S/m to hydrogels. Figure 2.3 provides a clear illustration of the chemical structure of hydrogels.

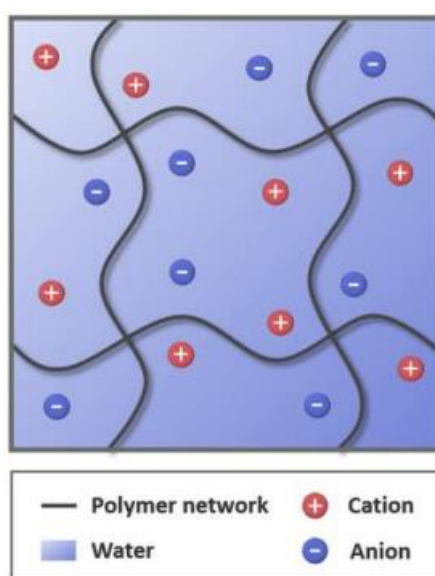


Figure 2.3: Chemical structure of hydrogel.

2.3 Types of Actuation

Actuation involves the conversion of electrical energy into mechanical force, enabling the movement of a machine. Actuators serve as essential components in both soft robots and traditional rigid robots, facilitating various movements. Several categories of actuation including electrically-responsive, magnetically-responsive, thermally-responsive, phot-responsive, pressure-driven, and explosive are discussed.

2.3.1 Electrically Responsive

2.3.1.1 Dielectric Elastomer Actuators

Dielectric elastomer actuators (DEAs) exploit the electromechanical properties of elastomeric materials. These actuators deform in response to an applied electric field, as the electrostatic forces between oppositely charged electrodes cause the elastomer to contract or expand (Pelrine et al., 2000). Figure 2.4 shows the deformation of DEAs with voltage application and Figure 2.5 shows various types of DEAs. DEAs offer remarkable actuation strains, fast response times, and low power consumption. They find applications in soft robotics, haptic interfaces, and biomimetic systems due to their high compliance and ability to generate large forces with minimal energy input (Polygerinos et al., 2015). DEAs are characterized by their ability to produce large deformations, making them suitable for applications requiring soft, human-like movements. These actuators have been used in the development of artificial muscles, soft grippers, and wearable devices for rehabilitation and assistance. DEAs can also be integrated into complex systems such as soft exoskeletons and prosthetic limbs, where their lightweight and energy-efficient nature offers significant advantages.

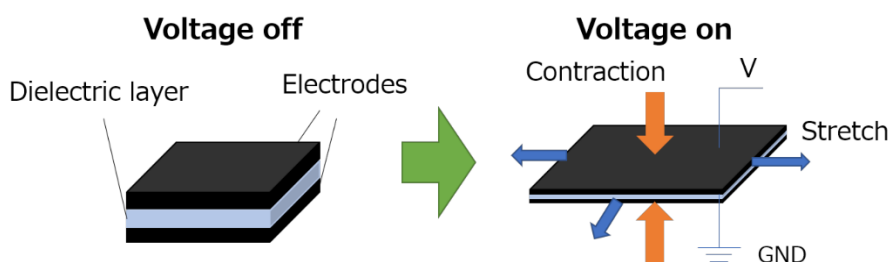


Figure 2.4: Deformation of DEAs. Reprinted with permission from copyright 2017 Springer Nature.

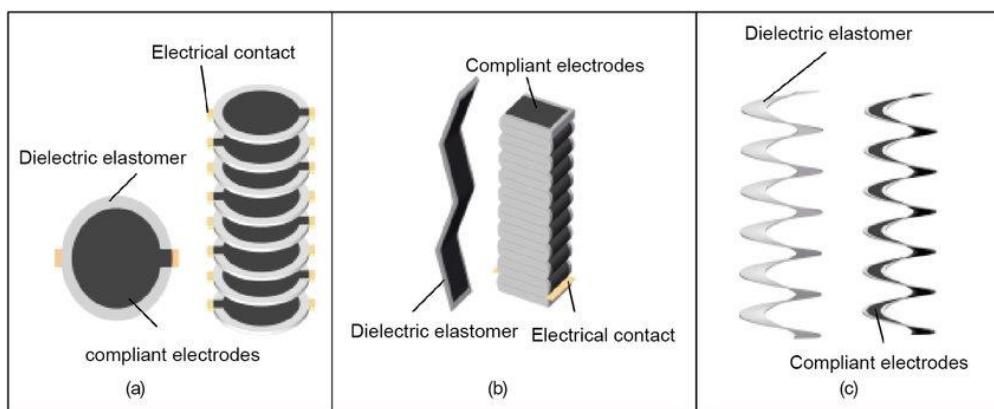


Figure 2.5: Types of DEAs. (a) Layer by layer stacked actuator; (b) folded actuator; (c) helical actuator. Reprinted with permission from copyright 2017 Springer Nature.

2.3.1.2 Mechanical/Servomotor

Mechanical or servomotor actuators rely on mechanical principles to generate motion or force. These actuators typically involve the conversion of electrical energy into mechanical motion through gears, cams, or other mechanical components (Trivedi et al., 2008). While not inherently soft, they can be integrated into soft robotic systems for specific applications requiring high force or precision, such as grippers, manipulators, and prosthetic limbs. Servomotor actuators offer robustness, reliability, and precise control, making them suitable for various industrial and research applications. Servomotor actuators are characterized by their high torque output and precise position control, making them suitable for applications requiring high force or accurate positioning. These actuators have been used in robotics, automation, and mechatronics for tasks such as manipulation, assembly, and machining. Servomotor systems often include feedback mechanisms such as encoders or sensors to ensure accurate positioning and control.

2.3.2 Magnetically Responsive

Magnetically responsive actuators utilize magnetic fields to induce motion or deformation in soft materials. These actuators may employ ferromagnetic or magnetorheological materials that change shape or stiffness in response to magnetic fields. By controlling the intensity and direction of magnetic fields,

these actuators can achieve precise and reversible actuation (Kim et al., 2013). They find applications in soft robotics, adaptive structures, and biomedical devices for tasks such as drug delivery, tissue engineering, and soft grippers. Figure 2.6 shows the several shapes of deformation for magnetically responsive actuators.

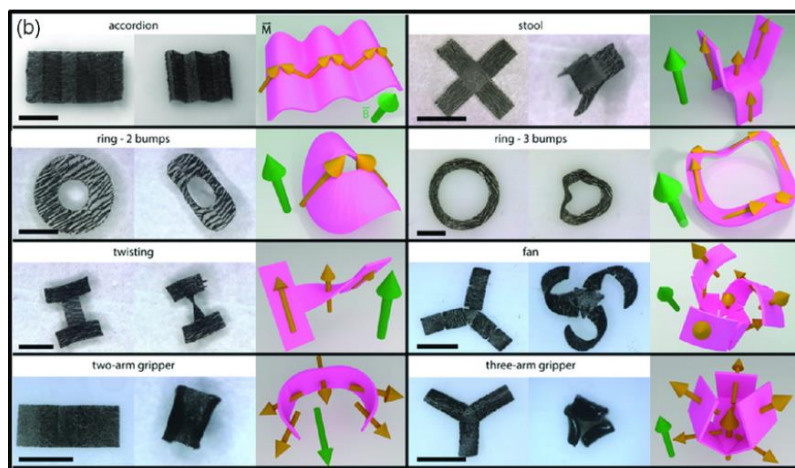


Figure 2.6: Shapes of deformation for the magnetically responsive actuator. Reprinted with permission from copyright 2016 IEEE.

Magnetically responsive actuators offer several advantages, including remote actuation without physical contact, tunable actuation through magnetic field modulation, and compatibility with non-magnetic environments. They are particularly useful in applications where direct mechanical contact is undesirable or impractical, such as minimally invasive surgery, targeted drug delivery, and microscale manipulation (Baechle et al., 2013). Additionally, magnetically responsive actuators can operate in harsh environments, including underwater or inside the human body, where other actuation methods may be ineffective or hazardous. Overall, these actuators provide a versatile and robust solution for a wide range of engineering and biomedical applications, making them an area of active research and development.

2.3.3 Thermally Responsive

2.3.3.1 Shape Memory Polymer

Shape memory polymer (SMP) actuators exhibit shape memory behaviour due to reversible phase transitions in polymer chains. Upon heating or cooling,

SMP actuators undergo a transition between temporary and permanent shapes, enabling controlled actuation (Lendlein & Langer, 2002). Figure 2.7 shows the state of SMP under different temperatures. SMP actuators offer advantages such as lightweight, low-cost, and tunable activation temperatures. They are used in soft robotics, biomedical devices, and smart materials for applications such as grippers, stents, and adaptive structures.

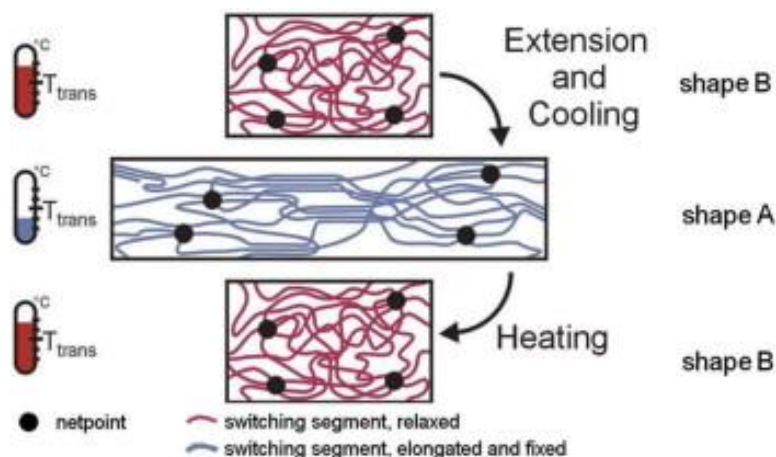


Figure 2.7: State of SMP under different temperatures. Reprinted with permission from copyright 2023 Springer Nature.

Shape memory polymer actuators provide a versatile and customizable solution for actuation in various engineering and biomedical applications (Wurth et al., 2017). Their ability to undergo large deformations while recovering their original shape upon stimulus removal makes them suitable for applications requiring reversible and programmable motion. Additionally, SMP actuators can be tailored to exhibit specific activation temperatures and mechanical properties, allowing for precise control and optimization for specific tasks. Ongoing research in SMP materials and processing techniques is expected to further enhance their performance and expand their applicability in areas such as soft robotics, wearable devices, and minimally invasive medical procedures.

2.3.3.2 Liquid Crystal Elastomer

Liquid crystal elastomer (LCE) actuators undergo reversible shape changes in response to thermal stimuli. These materials combine the properties of liquid

crystals and elastomers, enabling precise control over actuation behaviour through temperature modulation (White et al., 2015). Figure 2.8 shows the deformation of LCE at low and high temperatures. LCE actuators exhibit large deformations, fast response times, and programmable anisotropy, making them suitable for applications requiring complex and reversible shape changes. They find applications in soft robotics, optics, and adaptive structures for tasks such as tunable lenses, soft actuators, and morphing surfaces.

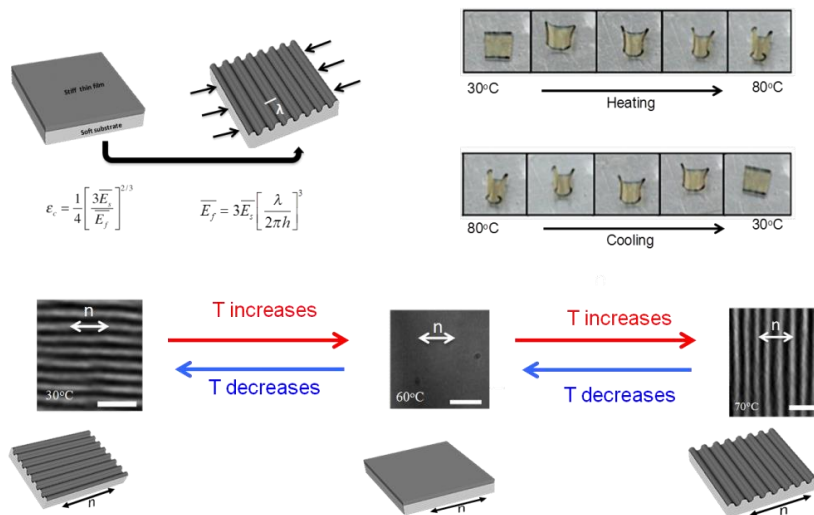


Figure 2.8: Deformation of LCE at low and high temperatures. Reprinted with permission from copyright 2017 Springer Nature.

Liquid crystal elastomer actuators offer unique capabilities for dynamic and reversible actuation in soft robotic systems and adaptive materials (Marchese et al., 2015). Their ability to respond to thermal stimuli with large and controllable deformations makes them suitable for applications requiring programmable and multifunctional motion. Additionally, LCE actuators can be engineered to exhibit specific mechanical properties and actuation behaviours, allowing for tailored performance in various applications. Ongoing research in LCE materials design and processing techniques is expected to further advance their capabilities and enable new functionalities, such as shape-changing surfaces, tunable optics, and responsive materials for biomedical applications.

2.3.3.3 Synthetic Hydrogel

Synthetic hydrogel actuators respond to changes in temperature by swelling or shrinking, resulting in mechanical deformation. These actuators are composed of crosslinked polymer networks capable of absorbing and releasing water in response to temperature variations (Li & Mooney, 2016). Synthetic hydrogel actuators offer advantages such as biocompatibility, tunable responsiveness, and stimuli-responsive behaviour. They are used in soft robotics, drug delivery systems, and tissue engineering for applications such as actuators, sensors, and scaffolds.

Synthetic hydrogel actuators provide a versatile and biocompatible platform for actuation and sensing in biomedical and soft robotic applications (Pelrine et al., 2000). Their ability to respond to environmental stimuli, such as temperature, pH, or solvent composition, enables dynamic and reversible motion in response to physiological cues. Additionally, synthetic hydrogels can be engineered to exhibit specific mechanical properties, such as stiffness, elasticity, and swelling behaviour, allowing for tailored performance in different applications. Ongoing research in hydrogel design and functionalization is expected to further enhance their capabilities and enable new applications in areas such as drug delivery, tissue engineering, and wearable devices.

2.3.4 Photo Responsive

2.3.4.1 NIR Light Driven

Near-infrared (NIR) light-driven actuators exploit the ability of certain materials to absorb NIR light and convert it into thermal energy, leading to actuation (Kim et al., 2018). NIR light-driven actuators enable precise and localized control over motion in response to light stimuli. Figure 2.9 shows the deformation of the NIR light-driven actuator. These actuators find applications in biomedical devices, optical systems, and soft robotics for tasks such as drug release, tissue manipulation, and optical switching.

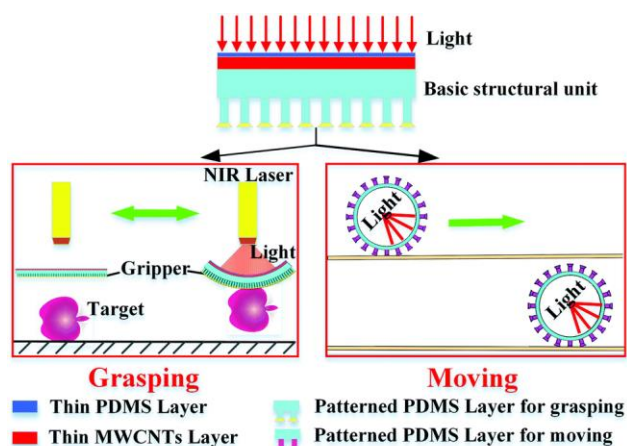


Figure 2.9: Deformation of NIR light-driven actuator. Reprinted with permission from copyright 2023 IEEE.

Near-infrared light-driven actuators provide a promising solution for actuation in biomedical and optical applications where precise control and compatibility with biological tissues are required (Kim et al., 2018). Their ability to respond to NIR light with rapid and reversible motion enables targeted and non-invasive manipulation *in vivo*. Additionally, NIR light-driven actuators offer the advantage of deep tissue penetration and minimal phototoxicity, making them suitable for applications in deep-brain stimulation, optogenetics, and photothermal therapy. Ongoing research in NIR-responsive materials and device integration is expected to further advance the capabilities and enable new applications of these actuators in biomedical imaging, diagnostics, and therapeutics.

2.3.5 Pressure Driven

2.3.5.1 Pneumatic

Soft pneumatic actuators (SPAs) harness compressed air or gas to induce motion or deformation in soft materials (Mosadegh et al., 2015). By regulating the flow of pressurized air through pneumatic networks or chambers integrated within soft structures, these actuators generate mechanical forces. Figure 2.10 shows the soft pneumatic actuator at its unpressurised state and pressurised state. One key advantage of SPAs is their inherent compliance, which allows for safe interaction with humans and delicate objects. Unlike traditional rigid actuators, SPAs can deform and conform to their environment, reducing the

risk of injury or damage during interaction. This compliance enables SPAs to perform tasks near humans or within confined spaces, making them ideal for applications such as assistive devices, wearable robotics, and human-robot collaboration (Rus and Tolley, 2015).

Additionally, SPAs offer tunable stiffness and controllable motion, allowing for precise and adaptive actuation. By adjusting parameters such as air pressure, chamber geometry, or material properties, the behaviour of SPAs can be tailored to suit specific tasks and environments. This flexibility makes SPAs suitable for a wide range of applications, from soft grippers and manipulators to locomotion systems and rehabilitation devices (Polygerinos et al., 2015). Another advantage of SPAs is their simplicity and ease of fabrication. Compared to traditional rigid actuators, which often require complex mechanisms and manufacturing processes, SPAs can be fabricated using relatively simple techniques such as 3D printing or molding. This simplicity not only reduces costs but also facilitates rapid prototyping and customization, allowing researchers and engineers to iterate designs quickly and efficiently (Martinez et al., 2013). Despite these advantages, SPAs also face some limitations. One common challenge is achieving precise control and coordination of multiple actuators within a soft robotic system. As SPAs rely on pneumatic pressure for actuation, coordinating the timing and sequencing of multiple actuators can be complex, especially in highly dynamic or unstructured environments.

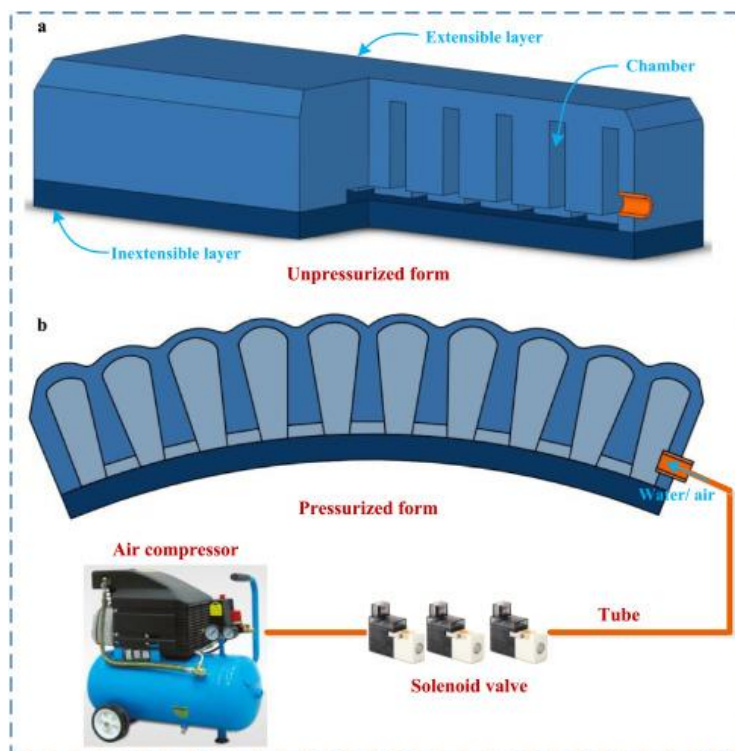


Figure 2.10: Unpressurised state and pressurised state of soft pneumatic actuator. Reprinted with permission from copyright 2016 IEEE.

2.3.5.2 Hydraulic

Hydraulic actuators transmit force through the circulation of a liquid, commonly water or oil, to induce motion in soft materials (Wang et al., 2018). They utilize hydraulic pressure to pressurised the cavities within soft structures, producing actuation. Figure 2.11 shows the pressurisation of a soft hydraulic actuator. Hydraulic actuators offer high power density and are capable of generating substantial forces, rendering them suitable for applications demanding heavy load capacities (Gorissen et al., 2017). In soft robotics, aerospace, and industrial automation, hydraulic actuators play pivotal roles in tasks such as manipulation, locomotion, and load lifting. Their robustness, efficiency, and adaptability make them indispensable in scenarios requiring reliable and high-performance actuation.

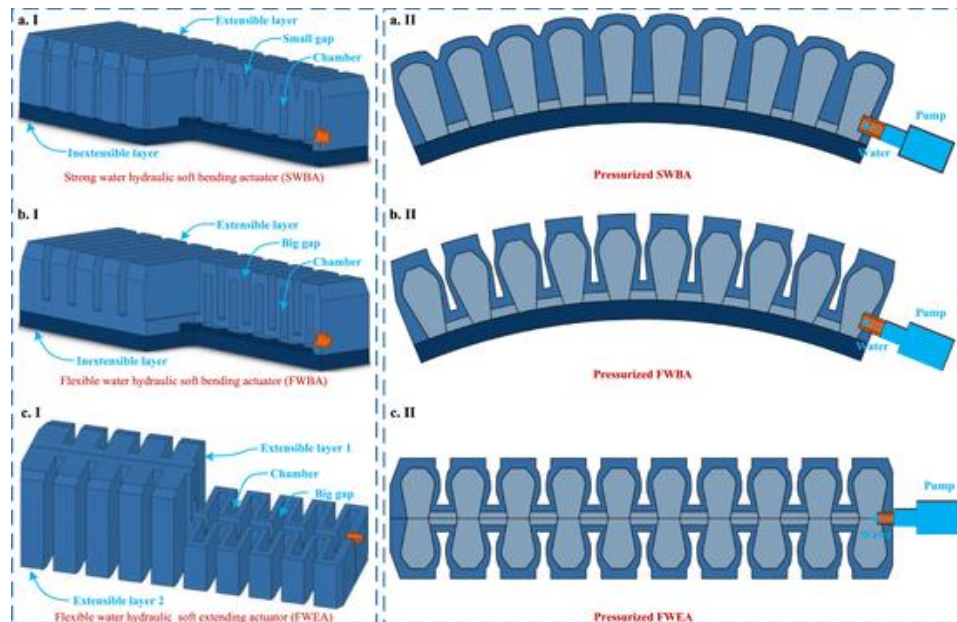


Figure 2.11: Pressurisation of a soft hydraulic actuator. Reprinted with permission from copyright 2016 IEEE.

2.4 Soft Actuator Structure

The design and structure of soft actuators play a crucial role in their functionality, performance, and versatility. Several types of structures have been explored in soft robotics, including ribbed, cylindrical, and pleated designs, each offering unique advantages and applications.

2.4.1 Ribbed Structures

Ribbed structures in soft actuators consist of a series of parallel ribs or ridges arranged along the length of the actuator. These ribs provide structural support and prevent buckling or collapse during deformation. Ribbed structures offer enhanced bending stiffness and directional control, making them suitable for applications requiring precise manipulation and force transmission (Marchese et al., 2015). They find applications in soft grippers, manipulators, and robotic arms for tasks such as grasping, lifting, and object manipulation. The discrete ribs allow for localized reinforcement and tailored mechanical properties, enabling efficient energy transfer and motion amplification in soft robotic systems. The ribbed segment comprises three layers, as depicted in Figure 2.12. In its un-actuated state (A), the segment remains unaffected. However, upon actuation (B), the segment undergoes pressurization of the channel group. The

segment delineates into distinct components, including the soft elastomer (a), embedded fluidic channels (b), inextensible yet flexible constraint (c), embedded fluid transmission lines (d), and ribbed structures (e) (Marchese et al., 2014).

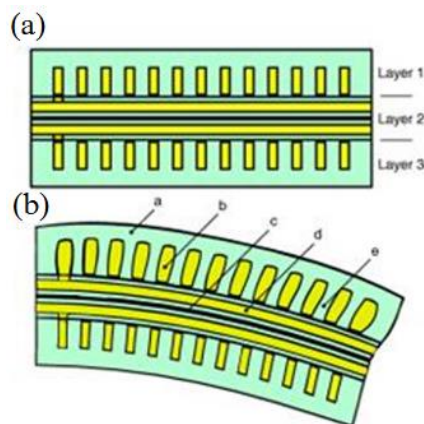


Figure 2.12: Concept of a ribbed segment. (a) Before the air chambers are pressurized (b) After the air chambers are pressurized. Reprinted with permission from copyright 2012 John Wiley and Sons.

2.4.2 Cylindrical Structures

Cylindrical structures are characterized by their tubular or cylindrical shape, offering uniform deformation and omnidirectional actuation. These structures are typically composed of elastomeric materials with varying degrees of compliance and stiffness. Cylindrical soft actuators can undergo axial elongation, radial expansion, or twisting motion, depending on their design and actuation mechanism. The cylindrical segment consists of two fluid-filled channels interconnected and positioned at the outermost layer, as illustrated in Figure 2.13. Upon pressurizing one of the channels, the embedded channel bends, curving and extending. The inner layer, depicted in Figure 2.13, comprises stiff rubber, serving as an inextensible constraint. This segment is segmented into six components: crush-resistant silicone inlets (a), soft silicone rubber outer layer (b), expanding embedded fluidic channels (c), stiffer silicone inner layer (d), soft endplates (e), and internal tubing bundle (f) (Martinez et al., 2013). They find applications in soft actuators, pneumatic muscles, and wearable devices for tasks such as locomotion, gripping, and

sensing (Ilievski et al., 2011). Cylindrical structures provide simplicity, scalability, and versatility in soft robotic design, allowing for easy integration into complex systems and environments.

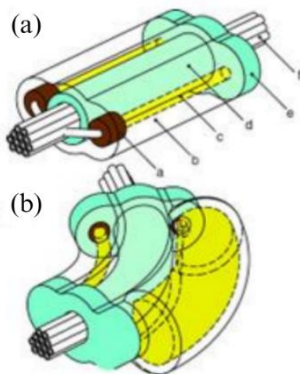


Figure 2.13: Concept of cylindrical segment. (a) Before the channels are pressurized (b) After the channels are pressurized. Reprinted with permission from copyright 2012 John Wiley and Sons.

2.4.3 Pleated Structures

Pleated structures feature a series of accordion-like folds or pleats arranged along the length or circumference of the actuator. These pleats enable reversible expansion and contraction of the actuator, resulting in bending or twisting motion. Pleated structures offer high flexibility, compliance, and adaptability to various bending radii and curvatures (Gorissen et al., 2017). As depicted in Figure 2.14, the hollow channels are interconnected with a central channel accessible through a front inlet. Upon pressurization, one of the pleats undergoes balloon-like expansion of the thin exterior skin. The collective expansion of all the pleats induces bending in the soft robots. The design of the pleated segment is categorized into four components: channel inlet (a), inextensible constraint layer (b), evenly divided gaps (c), and equal pleats (d) (Martinez et al., 2013). They find applications in soft robotics, biomedical devices, and morphing structures for tasks such as locomotion, manipulation, and shape-changing. Pleated structures can achieve complex motion profiles with minimal energy input, making them suitable for applications requiring agile and dexterous manipulation in confined spaces or irregular environments.

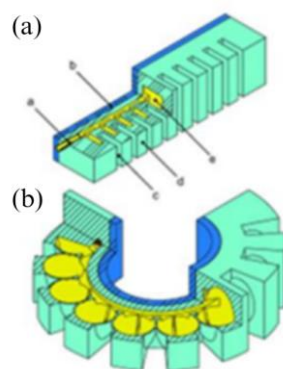


Figure 2.14: Concept of a pleated segment. (a) The cross-sectional area of the hollow channels before being pressurized (b) The cross-sectional area of hollow channels after being pressurized. Reprinted with permission from copyright 2012 John Wiley and Sons.

2.5 Locomotion Inspiration

This subchapter explores a diverse range of locomotion strategies inspired by animal movement. By drawing from nature's designs, researchers have sought to emulate the unique locomotive abilities observed in various species. These bio-inspired locomotion techniques encompass a spectrum of forms, from the slithering motion of snakes to the agile flight of birds. By studying and replicating these natural movement patterns, scientists aim to develop innovative robotics capable of navigating different environments with efficiency and adaptability. The exploration of animal-inspired locomotion represents a rich source of inspiration for advancing robotics technology towards more sophisticated and versatile designs.

2.5.1 Eel-Inspired

Nguyen & Ho (2022) experimented to study the anguilliform swimming performance of an eel-inspired soft robot. The soft pneumatic actuators in the eel robot mimic eel muscles by providing undulatory movement through pulse control signals with a suitable shifting phase. In the design of the soft eel robot, four pairs of soft actuators are used to construct the robot body. These actuators are controlled using pulse signals with appropriate shifting phases to deliver compressed air in sequence, creating a sinusoidal wave motion from

the head to the tail of the robot body. This design shown in Figure 2.15 allows the soft actuators to replicate the shape and motion characteristics of eel muscles, enabling the robot to achieve anguilliform swimming performance similar to that of natural eels.

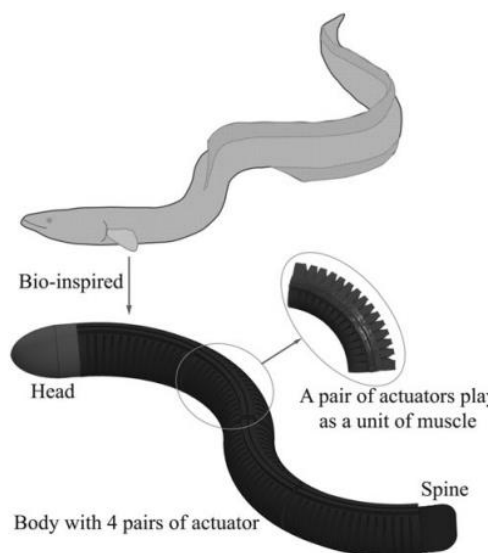


Figure 2.15: Eel-inspired design. Reprinted with permission from copyright 2017 Mary Ann Liebert, Inc.

The generated thrust force of the robot is positively correlated with the beat frequency. The suitable frequency range for the soft robot eel to swim efficiently was found to be between 0.83 to 1.67 Hz. The optimum frequency is 1.25 Hz and the robot was able to achieve a cost of transport (COT) of 10.72 and velocity at 0.36 body length per second (BL/s). The air pressure applied to the actuators at different segments from the head to the tail of the robot body also influences swimming efficiency. Varying the air pressure can affect the propulsion and overall performance of the robot. The shifting phase of the control signal strongly affects the swimming speed and the COT of the robot. Optimal control signal shifting phases can lead to higher velocities and lower energy consumption, thus improving swimming efficiency. The design of the soft robot eel, including the materials used for construction, can impact its swimming efficiency. Optimizing the design and selecting suitable materials can enhance the robot's performance in water.

2.5.2 Frog-Inspired

A frog-inspired robot, shown in Figure 2.16, was designed by Fan et al. (2020), based on the idea of modular design, with the forelimb consisting of a connecting piece, shoulder joint, and flipper, and the hind limb composed of various components including a connecting piece, hip, knee, ankle joint, thigh, lower leg, and flipper. Different air pressures inside the articulated pneumatic soft actuators enabled coordinated movement of the limbs, mimicking the flexibility and adaptability of frog movements. Soft actuators were identified as key components in achieving motion in soft robots. By analysing the structure of natural organisms like frogs, researchers proposed new ways to design and analyse soft robots. The use of soft actuators contributed to the compactness, miniaturization, and lightweight properties of the robot, aligning with the characteristics of frog movements. The layout of each joint coordinate system in the robot was designed to mimic the hind limb and forelimb coordinate systems of frogs, enhancing the biomimetic nature of the robot's movement. The design of the flippers in the robot was inspired by the flexible flippers of frogs, allowing for one-way drainage mechanisms during propulsion and recovery phases. The flippers were structured to ensure sufficient contact area with the medium for generating driving force, similar to how frogs propel themselves in water.

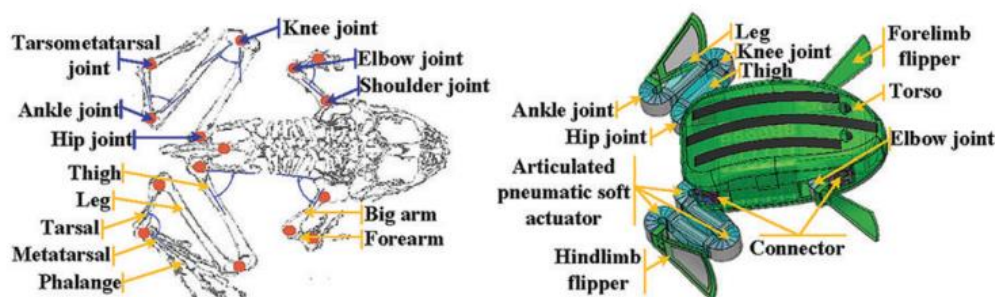


Figure 2.16: Frog-inspired design. Reprinted with permission from copyright 2020 Mary Ann Liebert, Inc.

The average propulsion speed during linear motion was measured to be 0.075 m/s. This speed indicates how fast the robot could move forward in a straight line, showcasing its ability to propel itself efficiently in a controlled manner. The average turning speed of the robot was recorded at 15°/s. This

speed represents the rate at which the robot could turn or change direction while swimming, demonstrating its agility and manoeuvrability in navigating through water environments.

2.5.3 Butterfly-Inspired

The butterfly-inspired swimming robot mimics the wing movements of butterflies for efficient underwater motion. These robots are designed with flexible wings to generate propulsion by mimicking the oscillatory motion of butterfly wings, offering a balance between manoeuvrability and energy efficiency. Zhu et al. (2018) developed a robot that minimized drag and enhanced manoeuvrability by using large, flexible wings to propel through low Reynolds number environments.

Soft materials like silicone and Ecoflex are commonly used to replicate the flexibility of butterfly wings. Advances in 3D printing enable lightweight, flexible wing designs that vary in stiffness for better propulsion and control (Liu et al., 2021). Materials such as shape memory alloys (SMAs) enhance performance by allowing controlled deformation during movement (Wang et al., 2019).

Effective actuation mechanisms, including pneumatic actuators and electroactive polymers (EAPs), replicate butterfly wing flapping. Pneumatic actuators enable precise control of flapping frequency and amplitude, creating smooth, energy-efficient propulsion (Wang et al., 2019). These robots rely on flapping and undulatory motion, offering flexibility and manoeuvrability in complex environments (Shen et al., 2020). Adjusting flapping parameters in real time helps them adapt to different swimming conditions, ideal for navigating coral reefs or underwater structures.

2.6 Hardware

Microcontrollers serve as the brains behind countless electronic devices, providing computation, control, and connectivity capabilities. Among the popular microcontrollers in the maker and IoT communities are the Arduino UNO and ESP32, each offering unique features and applications.

2.6.1 Arduino UNO

The Arduino UNO is a widely used open-source microcontroller board based on the ATmega328P chip. It features digital and analogue input/output pins, onboard memory, and a USB interface for programming and communication. The Arduino UNO is renowned for its simplicity, ease of use, and extensive community support. It is ideal for beginners and hobbyists interested in electronics, robotics, and automation projects (Banzi & Shiloh, 2014). The Arduino IDE (Integrated Development Environment) simplifies programming with a user-friendly interface and a vast library of pre-written code and examples. Arduino UNO's versatility makes it suitable for a wide range of applications, including home automation, sensor networks, and interactive art installations.

2.6.2 ESP32

The ESP32 is a powerful Wi-Fi and Bluetooth-enabled microcontroller developed by Espressif Systems. It features dual-core processing, low-power modes, and a rich set of peripherals, making it ideal for IoT (Internet of Things) applications. The ESP32 offers integrated Wi-Fi and Bluetooth connectivity, allowing seamless communication with other devices and the internet. It supports a range of wireless protocols and network configurations, enabling IoT devices to connect to local networks or cloud services (Srivastava & Singh, 2020). The ESP32 is commonly used in smart home devices, wearable technology, and industrial monitoring systems. Its advanced features, such as secure boot and encryption, make it suitable for applications requiring data privacy and security.

2.6.3 Micro Vacuum Air Pump and Micro Solenoid Valve

Micro vacuum air pumps and micro solenoid valves play crucial roles in various microfluidic and pneumatic systems, offering precise control and manipulation of fluids and gases at small scales. Micro vacuum air pumps are miniature devices designed to generate vacuum or negative pressure at microscale levels. These pumps utilize various mechanisms such as diaphragms, piezoelectric actuators, or electrostatic forces to create suction. They find applications in microfluidic devices for sample aspiration, cell

manipulation, and lab-on-a-chip systems (Mukhopadhyay et al., 2019). A study by Smith et al. (2017) investigated the design and fabrication of a micro vacuum air pump based on a piezoelectric actuator. The pump demonstrated efficient vacuum generation suitable for biomedical applications, such as microfluidic drug delivery and tissue engineering. Micro solenoid valves are miniature electromechanical devices used to control the flow of fluids or gases in microfluidic and pneumatic systems. These valves consist of a solenoid coil that, when energized, generates a magnetic field to actuate a plunger or diaphragm, thereby opening or closing the valve port. Micro solenoid valves offer fast response times, low power consumption, and precise flow control, making them ideal for lab-on-a-chip devices, analytical instrumentation, and medical diagnostics (Soper et al., 2016). In a study by Wang et al. (2018), a micro solenoid valve was integrated into a microfluidic platform for high-throughput cell sorting. The valve demonstrated rapid switching capabilities and compatibility with a wide range of biological samples, showcasing its potential for biomedical applications. Figure 2.17 shows a micro vacuum air pump with solenoid.



Figure 2.17: Micro vacuum air pump with solenoid.

2.7 Summary

This section explores recent advancements in soft robot design, focusing on innovations in materials, actuation methods, actuator structures, and locomotion strategies. In particular, butterfly-inspired locomotion was selected

for its advantages in lightweight design and compact size, making it ideal for underwater applications where manoeuvrability and agility are essential. The ribbed actuator structure was chosen for its smooth surface and reduced water resistance, which enhances the robot's efficiency by minimizing drag. A combination of pneumatic actuation and Ecoflex, a highly elastic silicone material, was selected for its capacity to achieve high-frequency actuation, enabling the generation of sufficient propulsion force to navigate through aquatic environments effectively. These design choices illustrate how bio-inspired approaches and material innovations are shaping the next generation of soft robotic systems, particularly in underwater settings.

CHAPTER 3

METHODOLOGY AND WORK PLAN

3.1 Introduction

This chapter outlines the components, materials, and methods used in the project. It covers the actuation mechanism applied to the soft robot, detailing the preparation, fabrication process, and structure design. Additionally, the chapter describes the assembly of the soft robot body and its actuator, providing a comprehensive overview of the steps taken to build and integrate these elements.

3.2 Soft Robot Design

The requirements for the soft robot in this project are small, soft, and able to swim. It takes the shape of a butterfly and produces thrust from the flapping of its wings. Figure 3.1 shows the 3D CAD drawing of the swimming soft robot proposed. It consists of a soft body and two attached bistable flexible ribbon frame-based wings. The H-shaped soft body consists of two soft bending actuators (45 mm (L) \times 20 mm (W) \times 10 mm (T)) with two spine-shaped pneumatic channels embedded within the top and bottom layer, combined by an elastic bridge in the middle. Figure 3.2 shows the pneumatic channels embedded within one soft-bending actuator. The soft bending actuator consists of three layers: upper, middle, and lower layers which are both elastic and stretchable. One end of the four parallel elastic strips (width, 3 mm) is joined to the sides of the soft body, then the other end of the strips are bonded together using adhesive, creating the bistable characteristic. The swimming mechanism is inspired by the fin or limbs of animals that push water backward and gain thrust from the drag exerted in the opposite direction, creating forward locomotion. The general equation of drag force is shown in Equation 3.1 as follows:

$$F_D = \frac{1}{2} C_D \rho A v^2 \quad (3.1)$$

where ρ is the density of fluid, v is the speed of the object relative to the fluid, C_D is the drag coefficient, and A is the cross-sectional area. Therefore, the hollow part of the wings is wrapped using thin elastic film to increase the surface area to produce a greater propelling force.

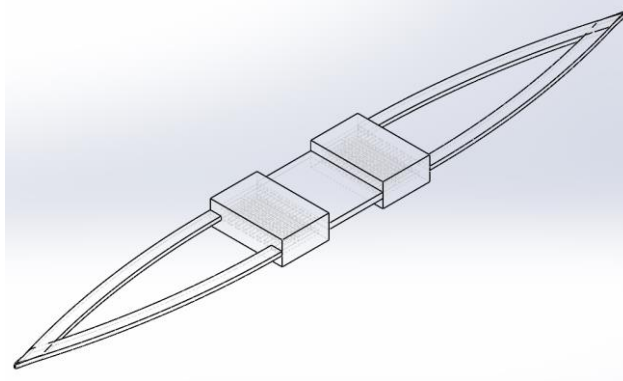


Figure 3.1: 3D CAD drawing of the soft robot.

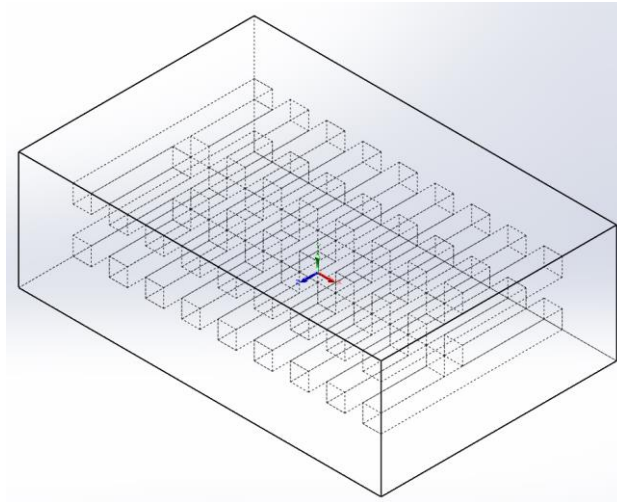


Figure 3.2: Pneumatic channels in one soft bending actuator.

Propelling motion with directional control can be achieved by pressurising the pneumatic channels, changing the state of the bistable flexible ribbon wings, hence creating propelling force. Alternatingly pressurising two of the upper channels followed by two of the lower channels can produce a straight propelling motion. Sequentially pressurising only one of the channels at a time will allow the soft body to change direction.

3.2.1 Materials

Ecoflex is chosen as the material for the three layers of the soft-bending actuator due to its distinct advantages. Ecoflex is a type of soft silicone rubber that offers exceptional flexibility, elasticity, and tear resistance. Table 3.1 shows that the Ecoflex 00-30 has lower Young's modulus value as compared to other elastic materials. One of the key advantages of Ecoflex is its similarity to human skin in terms of softness and texture, making it ideal for applications requiring close interaction with the environment or human users. Another advantage of Ecoflex is its ease of processing and customization. It can be easily poured, molded, or cast into complex shapes and geometries, allowing for the fabrication of intricate soft robotic structures. Ecoflex also enables the incorporation of additives or fillers to modify its mechanical properties, such as stiffness or damping characteristics, to suit specific application requirements. Furthermore, Ecoflex is durable and resistant to environmental factors such as moisture, heat, and chemicals, ensuring the longevity and reliability of the soft robot. Its resistance to wear and tear makes it suitable for outdoor or rugged environments where the robot may encounter rough terrain or harsh conditions. Figure 3.3 shows part A and part B of Ecoflex which are to be mixed with a ratio of 1:1.

Table 3.1: Comparison of Young's modulus of different materials.

Material	Young's Modulus
Ecoflex 00-30	125 kPa
PDMS (Polydimethylsiloxane)	500 kPa – 3MPa
Natural Rubber	1 – 2 MPa
Silicone Rubber	1 – 3 MPa
Polyurethane	10 – 50 MPa
Hydrogels	10 – 100 kPa



Figure 3.3: Part A and Part B of Ecoflex.

The mold for casting the soft bending actuator made of Ecoflex will be 3D printed using polylactic acid (PLA) filament. PLA offers several advantages such as ease of use, biodegradability, wide availability, nontoxicity, and good surface finish.

The material for the bistable flexible ribbon wings is a polyester sheet as shown in Figure 3.4. The polyester sheet is chosen because it has high strength, is resistant to chemicals, is easy to fabricate, and is recyclable. The high tensile strength allows the wing to stay in shape after bending and twisting after the two tips of the ribbons joined together.

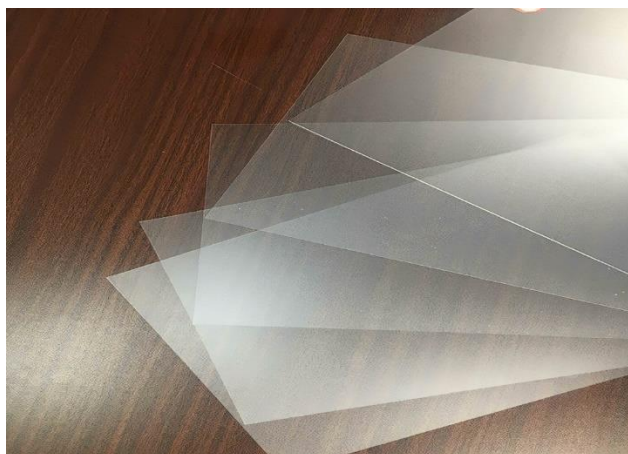


Figure 3.4: Polyester sheets.

3.2.2 Structure

The soft-bending actuator is designed to have a ribbed structure. This is because the ribbed structure has advantages that are crucial to a swimming robot. Firstly, the smooth outer surface allows the robot to swim efficiently

with minimum influence from water resistance and turbulence. Besides, unlike the pleated structure, the ribbed structure has reduced the risk of pneumatic channel kinking and improved durability. Another advantage of the ribbed structure is that the rib spacing, height, and geometry can be adjusted to achieve the optimum swimming performance.

3.2.3 Actuation

The actuation method used in the proposed design of the swimming soft robot is pneumatic actuation. Firstly, the lightweight air allows the soft robot to float on the water surface easily. Besides, pneumatic actuation is clean as compared to other methods such as hydraulic actuation which is susceptible to leakage. As the swimming soft robot is to be deployed in water, the possibility of leakage should be avoided to prevent pollution. Figure 3.5 and Figure 3.6 show the 12 V DC electric micro vacuum air pumps, and micro solenoid valves to be used in this project. The dimensions of the pneumatic tube to be used are 4 mm × 2.5 mm (outer diameter × inner diameter) to match the small pneumatic channels in the small swimming robot.



Figure 3.5: 12 V DC micro vacuum air pump.



Figure 3.6: Micro solenoid valves.

The micro vacuum air pumps will stay powered and the micro solenoid valves will be switched on and off to control the pressurisation of pneumatic channels in the soft bending actuator.

3.2.4 Control and Electronics

Arduino UNO board, as shown in Figure 3.7, is selected to be the controller of the small swimming soft robot. It is responsible for controlling the sequence of pressurisation and depressurisation of the robot through logic signals sent to the solenoid valve. A 4-channel 12 V Active Low shown in Figure 3.8 will be used to isolate the low-current circuit such as the Arduino, from the high-current circuit such as the DC power supply and solenoid valves. On the input side of the relay, the "GND" terminal should be linked to the "Ground (GND)" of the Arduino UNO, while the "VCC" terminal needs to be connected to the "Vin" of the Arduino UNO board. Subsequently, the inputs labelled "IN1" and "IN2" should be connected to the analogue pins, specifically "A1" and "A2" of the Arduino UNO. The relay can function as either Normally Opened (NO) or Normally Closed (NC) depending on how the device is connected in the output section of the relay. Figure 3.9 shows the pneumatic schematic diagram proposed.



Figure 3.7: Arduino UNO board.

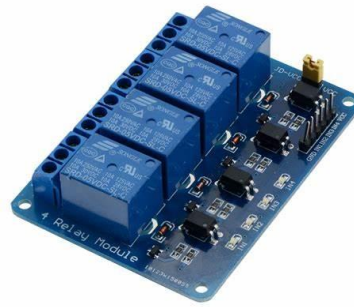


Figure 3.8: 4-channel relay.

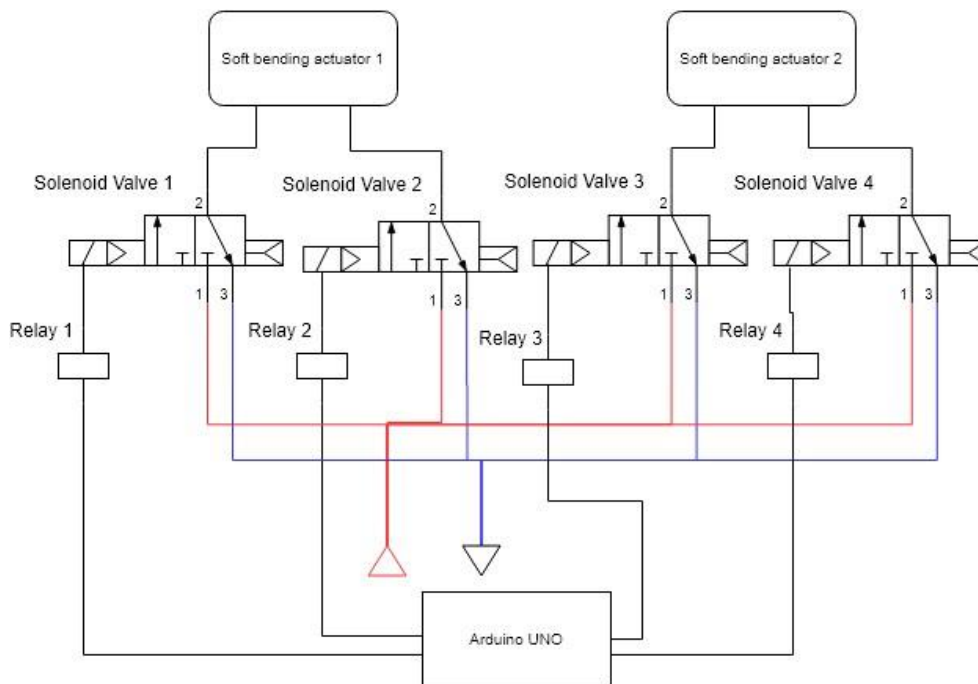


Figure 3.9: Pneumatic schematic diagram.

3.3 Fabrication

The fabrication plan for the swimming soft robot is summarised in a flowchart as shown in Figure 3.10. Two prototypes were fabricated in this project, each serving distinct purposes in the development and validation of the soft robot's swimming capabilities. The first prototype, as shown in Figure 3.11, was specifically designed to swim in a straight line and was instrumental in determining the optimum parameters for efficient swimming, such as actuation frequency and air pressure. By experimenting with various settings, this prototype allowed for fine-tuning of the soft robot's swimming performance.

The second prototype, as shown in Figure 3.12, was built to validate directional control. It was equipped with additional features to facilitate turns and manoeuvrability, enabling the robot to change its swimming direction with precision. This prototype was essential in proving the feasibility of the robot's ability to alter its path in water, providing critical insights for improving the overall design and control algorithm.

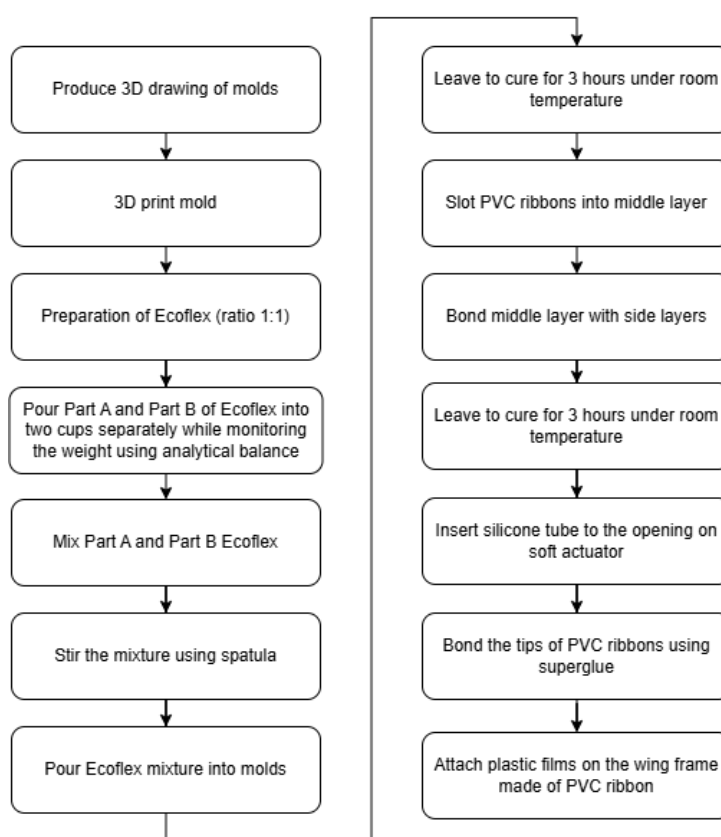


Figure 3.10: Flowchart of fabrication plan.



Figure 3.11: First prototype with single actuation body.

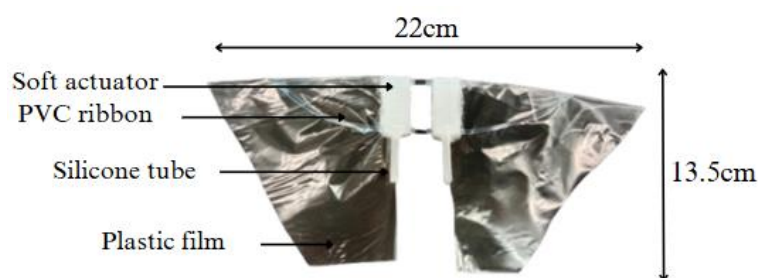


Figure 3.12: Second prototype with two actuation bodies.

3.3.1 Preparation of Mold

A mold for casting the Ecoflex is designed using SOLIDWORKS software. The cavity part in the designed actuator corresponds to the extruded part in the mold and vice versa. The mold is to be printed by a 3D printer using PLA filaments. The mold designs are shown in Figure 3.13.

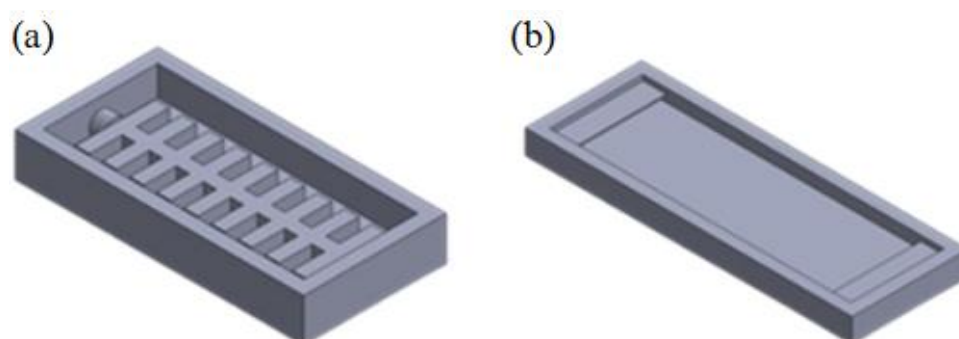


Figure 3.13: Mold for (a) side layers and (b) middle layer.

3.3.2 Ecoflex Casting and Assembly Process

Several pieces of equipment and materials were carefully prepared to ensure a smooth casting process. Essential items included Ecoflex Part A and Part B, a mold, a spatula, gloves, and an analytical balance. The required volume of Ecoflex Parts A and B was measured using the analytical balance, with the components mixed at a precise 1:1 ratio. Continuous stirring was performed during the mixing process to eliminate air bubbles, ensuring a smooth, even consistency.

The mixed Ecoflex was then evenly poured into both the top and base molds and left to cure at room temperature. The curing process was expected to take approximately three hours, after which the Ecoflex could be carefully peeled away from the mold. This process resulted in five distinct parts: two

upper layers, two lower layers, and one middle or bridge layer. Due to the symmetrical design, the upper and lower layers were identical, collectively referred to as the side layers.

As shown in Figure 3.14, the assembly process began by slotting two PVC ribbons into the middle layer. The middle and side layers were then bonded together using uncured Ecoflex, ensuring a secure and flexible connection. Silicone tubes were inserted into the soft body to enable pneumatic actuation. To finalize the structure, the tips of the ribbons were bonded with superglue for added reinforcement, and plastic films were attached to the ribbon frame, completing the construction of the soft robot body. This method provided a strong, durable structure while maintaining flexibility for optimal actuation performance.

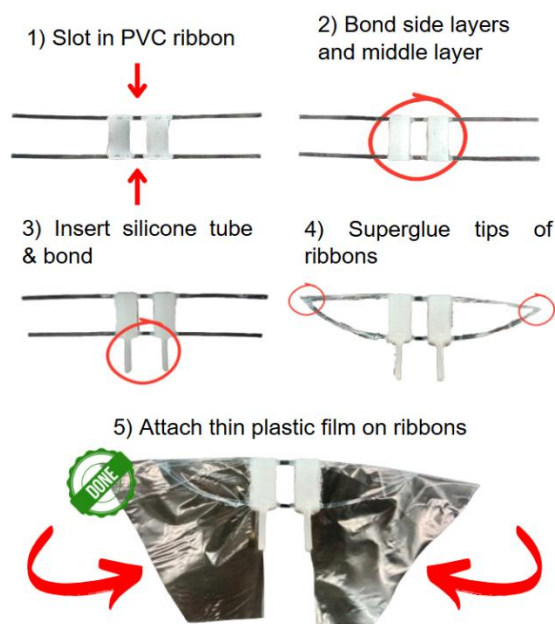


Figure 3.14: Assembly process.

3.3.3 Constructing the Electrical and Pneumatic Circuit

The power supply provides energy to the Arduino UNO development board and other electrical components within the circuit. A buck converter is used to step down the 12V input from the power supply to 5V, ensuring compatibility with the various electrical components. A hardware switch is integrated to regulate the power supplied to the DC pumps, enabling manual control over their operation. The system's relays manage the activation and deactivation of

micro solenoid valves, which in turn direct the flow of pressurized air into and out of the soft actuator. Depending on the pneumatic tubing configuration, the micro DC pumps are capable of either inflating the soft actuator by pumping pressurized air or generating a vacuum to create a low pressure, offering precise control over the actuation of the soft robot. The physical setup of the circuit is shown in Figure 3.15.

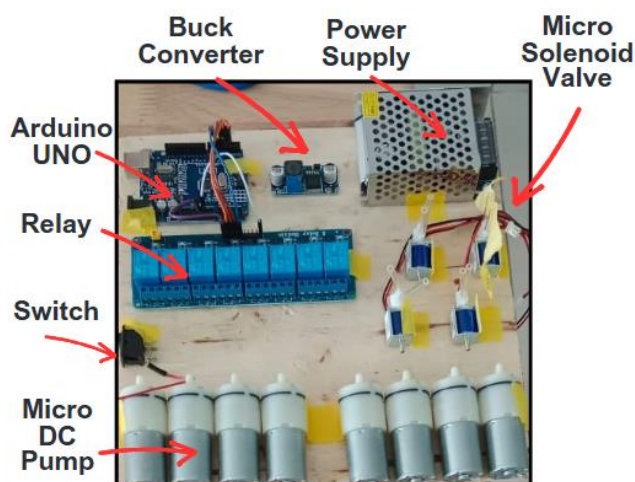


Figure 3.15: Electrical and pneumatic circuit.

3.4 Experiment Procedures

Firstly, the ability of the soft actuator to float on water surface was validated as shown in Figure 3.16. However, the actuator could not effectively maintain its orientation due to unsymmetrical deformation. Therefore, a pair of bistable wing constructed using PVC ribbons and plastic films was added to the soft actuator to form the first prototype.



Figure 3.16: Soft actuator floating on water surface from (a) side view and (b) isometric view.

As shown in Figure 3.17, the first soft robot prototype was tested for its swimming capabilities in a 22-litre storage box. Initially, its ability to swim in a straight line was validated. Following this, the experiment was repeated under varying actuation frequencies and pump voltages to determine the optimal frequency and voltage for performance. Finally, directional control was tested on the second prototype and validated using a second prototype equipped with four pneumatic chambers, demonstrating its manoeuvrability and enhanced control as shown in the setup in Figure 3.18.



Figure 3.17: Setup for first prototype swimming straight.

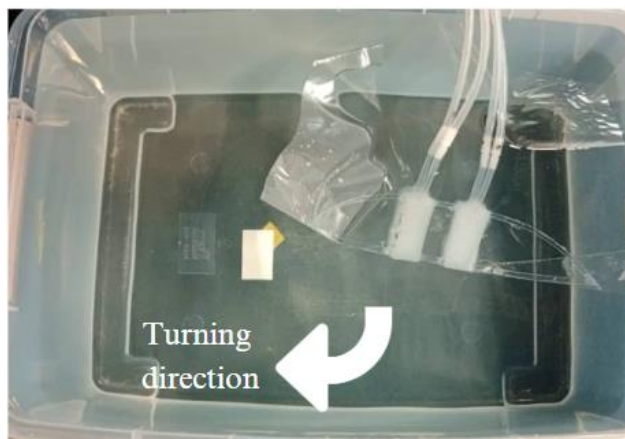


Figure 3.18: Setup for second prototype turning right.

3.5 Gantt Chart

The project activities carried out for FYP1 and FYP2 are shown in Table 3.1 and Table 3.2. All activities and milestones were able to be completed within schedule.

Table 3.2: Gantt Chart for FYP 1.

Gantt Chart Part-1															
No.	Project Activities	W1	W2	W3	W4	W5	W6	W7	W8	W9	W10	W11	W12	W13	W14
M1	Problem formulation & project planning	■	■												
M2	Literature review & data gathering		■	■	■	■	■	■							
M3	Simulation of soft robot model in COMSOL Multiphysics							■	■	■	■	■			
M4	Preliminary prototype building and testing											■	■	■	■
M5	Finalise results, report writing, and presentation											■	■	■	■

Table 3.3: Gantt Chart for FYP 2.

Gantt Chart Part-2															
No.	Project Activities	W1	W2	W3	W4	W5	W6	W7	W8	W9	W10	W11	W12	W13	W14
M1	Learning Experiment Setup	█	█												
M2	Prototype Fabrication and Testing		█	█	█	█	█	█	█						
M3	Data Analysis and Report Writing								█	█	█	█	█	█	
M4	Presentation and Report Submission													█	█

3.6 Summary

This chapter discusses the design of the soft robot, the fabrication work plan, the electrical and pneumatic circuits, as well as the experimental setup and procedures. Each section outlines the key steps and considerations involved in constructing the robot, integrating its electrical and pneumatic systems, and conducting tests to evaluate its performance.

CHAPTER 4

RESULTS AND DISCUSSION

4.1 Introduction

This chapter begins by presenting the results from the simulation, which visualizes the deformation of the soft actuator when the upper chamber is inflated with pressurized air. Following the simulation analysis, the deformation characteristics of the actual prototype are examined and compared. The chapter then moves on to validate the soft robot prototype's ability to swim in a linear path on water surface. A comprehensive analysis of the robot's swimming performance under various parameters, such as different inflation frequencies and air pressure levels, is conducted and discussed. The robot's ability to alter its direction during swimming is then evaluated and confirmed. Finally, the chapter concludes by validating the control algorithm designed to change the swimming direction of the soft robot using three push buttons, ensuring precise manoeuvrability in different conditions.

4.2 Simulation

Figure 4.1 illustrates the deformation of the soft bending actuator under varying pressures applied to the upper pneumatic channels. The simulation results reveal a direct correlation between the pressure levels and the extent of displacement and bending in the actuator. As pressure increases, the actuator experiences greater deformation due to the force exerted on the inner boundary of the channels, governed by the equation $F = PA$, where F is the force, P is the pressure, and A is the area. The force exerted by the pressurized air creates a bending moment, leading to bending stress on the soft actuator. In this scenario, the upper section of the actuator is subjected to tensile stress, while the lower section experiences compressive stress. The bending stress (σ) can be calculated using Equation 4.1:

$$\sigma = \frac{My}{I} = \frac{Ey}{R} \quad (4.1)$$

Where:

σ = Bending stress (Pa or N/m²)

M = Bending moment applied to the beam (N·m)

y = The perpendicular distance of a specific point on the beam's cross-section from its neutral axis (m)

I = The area moment of inertia of the beam (m⁴)

E = Modulus of Elasticity (Pa or N/m²)

R = Radius of Curvature (m)

Ideally, the bending of the soft actuator would be symmetrical, given its symmetric design along both the x and y axes. However, in the simulation, an asymmetrical bending was observed. This was due to the requirement in the COMSOL Multiphysics software to define a fixed constraint at one surface of the actuator, with the left surface being selected as the fixed point in this case. Consequently, the parameter “y” used in the bending stress calculation is affected, as the neutral axis is shifted to the leftmost fixed surface instead of the centreline of the actual prototype.

When the lower chamber is pressurized, the actuator will exhibit a similar bending pattern, but in the opposite direction due to the actuator's symmetric structure. These simulation results confirm the effectiveness of the proposed actuation mechanism and the associated locomotion algorithm. For the physical prototype, four pneumatic chambers within the soft actuators can be pressurized in sequence and in combination to execute specific movements, such as swimming in a straight line or changing direction.

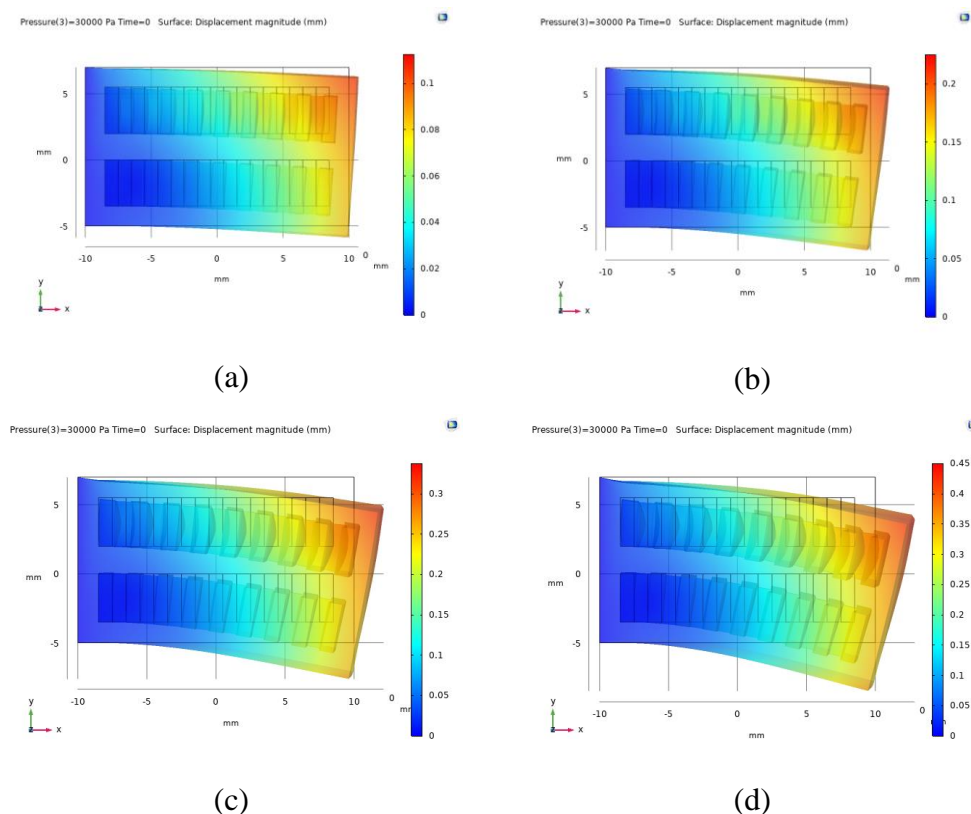


Figure 4.1: Deformation of the soft bending actuator under pressure (a) $P = 1$ MPa (b) $P = 2$ MPa (c) $P = 3$ MPa (d) $P = 4$ MPa.

4.3 Characterisation

Figure shows a soft actuator undergoing deformation due to pressurization in its upper pneumatic chamber. The soft actuator has a segmented, flexible design, made of a silicone-based material such as Ecoflex, which allows for controlled movement when inflated. When the upper pneumatic channel is pressurized, the air fills the chambers, causing them to expand and exert force on the actuator's inner walls. Due to the asymmetrical placement of the pneumatic channels, the actuator bends downward as the upper side of the structure extends, while the lower side contracts. This differential in pressure causes a curvature, as shown in Figure 4.2, where the actuator bends in the direction opposite to the pressurized side. The degree of bending depends on factors such as the pressure applied to the upper chamber, the material properties of the soft actuator, and the chamber's design, such as wall thickness and flexibility. Referring to Figure 4.3, the graph of soft actuator bending angle versus voltage reveals a nonlinear relationship where the

actuator bends more as voltage increases, but the rate of bending diminishes at higher voltages. Initially, small increases in voltage lead to more substantial gains in bending angle, but as the voltage approaches higher values, the incremental increase in bending angle becomes less pronounced, indicating a saturation effect. This behaviour is typical of soft actuators, where the material and design characteristics cause the bending angle to approach a maximum limit as voltage continues to rise.



Figure 4.2: Deformation of the soft actuator.

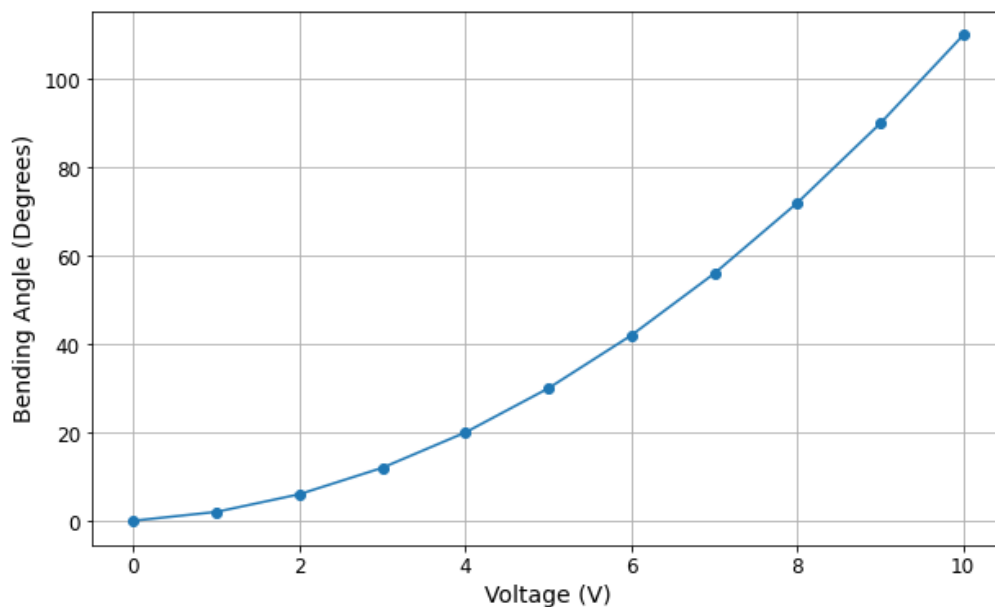


Figure 4.3: Graph of bending angle vs pump voltage.

In short, the deformation observed in the actual soft actuator closely aligns with the results obtained from the simulation. Both the simulation and the physical prototype exhibit similar bending behaviour when the upper pneumatic chamber is pressurized, confirming the accuracy and reliability of the simulation model in predicting the actuator's real-world performance.

4.4 Swimming Performance

4.4.1 Linear Swimming Motion

The experiment to validate the first soft robot prototype's ability to swim in a straight line was conducted using a 22-liter tank. As depicted in Figure 4.4 and Figure 4.5, the soft robot started at the designated point at time $t = 0$ s and successfully reached the finish point at $t = 10$ s, covering a 25 cm distance in a linear path at voltage of 12 V and frequency of 2.5 Hz. The robot's ability to maintain a straight trajectory was primarily due to the synchronized actuation of its pneumatic chambers. By alternately inflating the upper and lower chambers, the robot was able to create a steady propulsion force that drove it forward in a straight line.

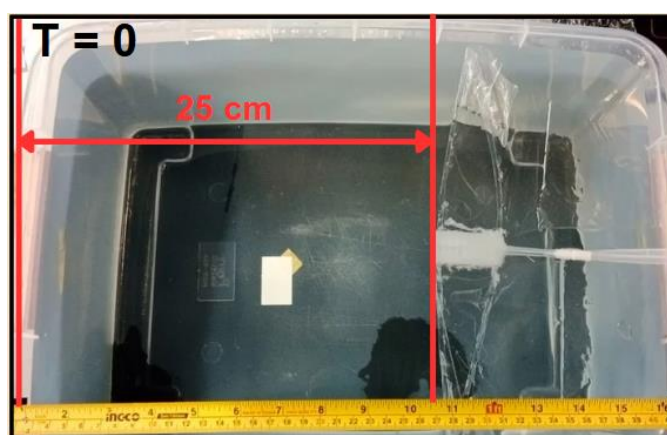


Figure 4.4: Soft robot position at $t = 0$ s.

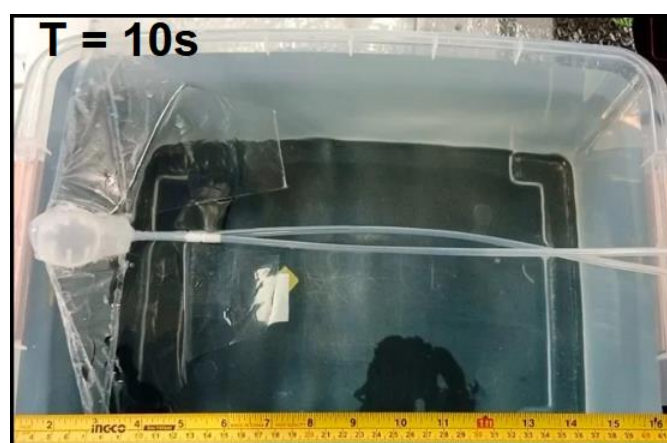


Figure 4.5: Soft robot position at $t = 10$ s.

4.4.2 Parameters for Optimum Swimming Performance in Linear Path

The first prototype's swimming performance was analysed at varying actuation frequencies and pump voltages. The pressure levels inside the top and bottom pneumatic chamber at high and low actuation frequencies were shown in Figure 4.6. Referring to Figure 4.7, the time taken to swim 25 cm was evaluated under different actuation frequencies. The results indicated that the robot's optimum swimming performance was achieved at an actuation frequency of 1.33 Hz at a constant pump voltage of 12 V, where the time taken to swim was minimized to 7 s. Higher frequencies resulted in diminished performance, due to insufficient inflation-deflation cycles, while lower frequencies could not generate enough propulsion force (Yang et al., 2019; Li et al., 2020). Referring to Figure 4.8, the optimum swimming performance was achieved using 11 V and 12 V pump voltage at a constant frequency of 1.33Hz. Besides, increasing pump voltage beyond 11 V did not improve the swimming speed significantly, indicating an upper threshold for efficient performance (Wang, 2018; Zhang and Liu, 2021).

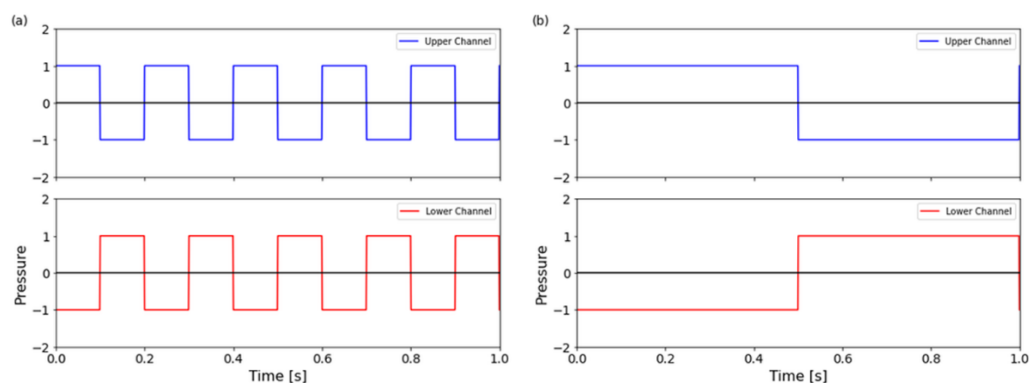


Figure 4.6: Pressure level in upper and lower pneumatic chamber at (a) 5 Hz and (b) 1 Hz.

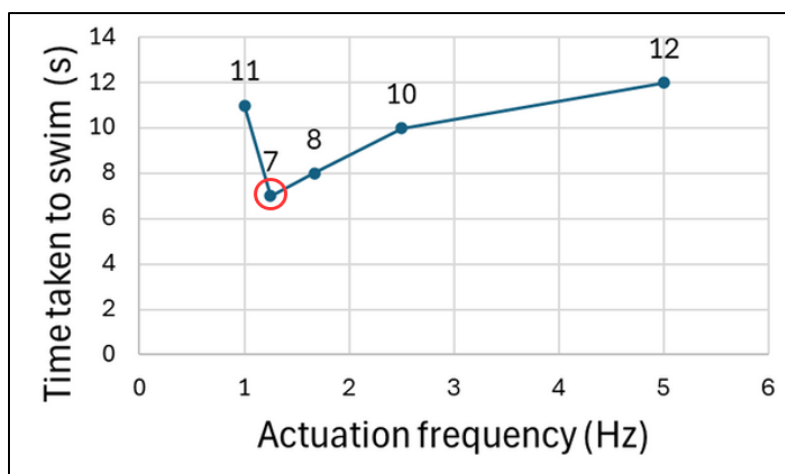


Figure 4.7: Time taken to swim in linear path for different actuation frequencies with optimum actuation frequency circled.

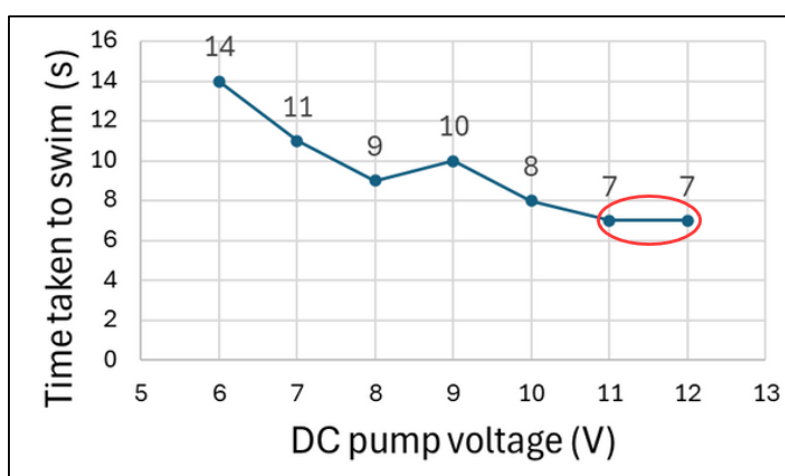


Figure 4.8: Time taken to swim in linear path for different pump voltages with optimum pump voltages circled.

4.4.3 Directional Control

The second prototype's ability to change direction was validated through experiments where the robot successfully demonstrated turning manoeuvres. As shown in Figure 4.9 (a), the robot, when at rest, could alter its direction by selectively inflating either the left or right chambers of its actuators. This controlled bending mechanism allowed the robot to pivot and make right or left turns as shown in Figure 4.9 (b). By pressurizing the right-side chambers, the robot turned left, and by inflating the left-side chambers, it turned right. The degree of turning was directly proportional to the inflation level and duration, enabling precise control of direction.



Figure 4.9: Robot (a) before turning right and (b) after turning right.

4.4.4 Swimming Algorithm

To achieve complete swimming control of enabling the robot to swim straight, turn left, or turn right, a custom algorithm was developed and implemented on an Arduino-based control system. Three push buttons were used to control the swimming direction: one for swimming straight, one for turning left, and one for turning right. When the "swim straight" button is pressed, the algorithm alternates the inflation between the upper and lower chambers of both actuators in a coordinated manner, ensuring forward propulsion. When the "turn left" button is pressed, only the right-side chambers are inflated, causing the robot to bend and turn left. Similarly, pressing the "turn right" button inflates the left-side chambers, resulting in a rightward turn. This algorithm, executed in real-time, ensures that the robot can navigate through water with high precision, mimicking biological swimming behavior.

The Arduino code, as attached in Appendix A, integrates the control of the pneumatic pumps and solenoid valves, executing the desired action based on the button pressed. The result is a simple, yet highly effective, control mechanism that allows the robot to autonomously swim in different directions in response to user inputs.

4.5 Biomechanics of Butterfly Stroke

The butterfly stroke is one of the most distinct and energy-intensive swimming styles, known for its unique undulating motion and symmetrical arm movements (Toussaint et al., 2006). As shown in Figure 4.10, it involves a coordinated sequence of movements, including simultaneous arm pulls, powerful leg kicks, and a body wave that propels the swimmer forward (Veiga

et al., 2014). This natural swimming mechanism can serve as an inspiration for the design and locomotion of a soft robot aimed at underwater applications. By replicating these motions, soft robots can benefit from efficient propulsion and manoeuvrability, while maintaining a fluid and graceful movement in water. Below is a detailed breakdown of the key biomechanics of butterfly locomotion and how they can be translated into soft robot design and swimming capabilities.

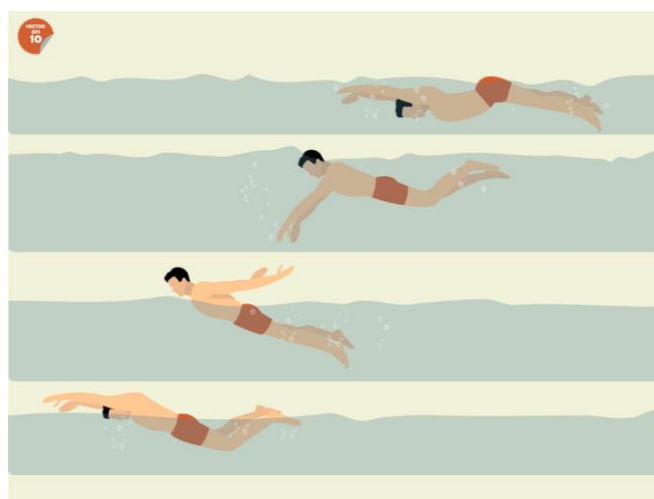


Figure 4.10: Butterfly stroke swimming style.

In human swimming, the butterfly stroke relies heavily on a wave-like motion that begins at the chest and travels down the body to the legs. This motion helps maximize propulsion and reduce drag in the water (Sanders et al., 1995). The soft robot prototype can replicate this wave-like movement by incorporating pneumatic or hydraulic actuators in different sections of its body, with alternating inflation and deflation patterns simulating the undulating motion. The wave motion will help generate forward thrust in water, improving speed and energy efficiency (Marchese et al., 2014). The body of the robot was designed with segmented soft actuators or bending muscles that are controlled in a sequential manner to create the smooth, flowing body movement seen in butterfly swimmers.

The arms in the butterfly stroke move symmetrically. Both arms reach forward in a sweeping arc, then simultaneously pull back in a powerful, coordinated manner. This pulling motion generates most of the propulsion

force, allowing the swimmer to surge forward (Chollet et al., 2006). The robot's body could feature dual soft actuator wings or fins on either side. When actuated simultaneously, they could mimic the sweeping arm motion, propelling the robot forward. The soft actuators was designed to bend and straighten in coordination to replicate the powerful "pull" phase. This enables efficient water displacement and propulsion (Kim et al., 2021). Pneumatic chambers or soft muscle segments can serve as the primary driving mechanism for these "arms," achieving high force output and rapid swimming when required.

The butterfly stroke employs a unique leg motion called the dolphin kick, where both legs move together in an undulating, wave-like pattern (Arellano et al., 2006). This kick starts from the hips and travels through the legs, helping to maintain forward propulsion between arm strokes. In a soft robot, the dolphin kick motion could be mimicked through flexible tail actuators or a compliant, wave-like rear section that moves in coordination with the front fins (Hu et al., 2020). A design with actuated tail fins or a flexible, undulating body similar to marine animals (like fish or dolphins) could generate the necessary thrust to keep the robot swimming efficiently, especially between strokes. The smooth, fluid motion would help the robot conserve energy while maintaining consistent movement in water.

Butterfly stroke swimmers rely on a highly synchronized rhythm between their arm strokes, body undulation, and leg kicks. This coordination is crucial for maintaining the right balance of propulsion and body positioning in the water (Sanders et al., 1995). A central control system was designed to synchronize the movements of various soft actuators (fins, body, and tail) for a smooth, rhythmic swimming action. The robot's control algorithm could be designed to mimic the timing and sequence of human butterfly stroke, ensuring that the robot maintains balance and stability while moving forward. By programming the actuators to inflate and deflate in a sequence similar to the butterfly swimming cycle, the robot could achieve coordinated swimming that conserves energy and optimizes propulsion.

The butterfly stroke involves reducing drag and maximizing thrust. The arms enter the water at a shallow angle, reducing water resistance, while the streamlined body position minimizes drag forces. A streamlined design for

the robot, with smooth surfaces and minimal sharp edges, could reduce hydrodynamic drag and allow it to glide efficiently through water. Flexible materials like silicone or Ecoflex used in the robot's body will naturally conform to water currents, further reducing resistance. The propulsion mechanism must strike a balance between power and efficiency, with soft actuators optimized for minimal drag while still generating sufficient thrust (Kim et al., 2021).

In butterfly stroke, swimmers adjust their body position and angle slightly to steer or maintain direction (Sanders et al., 1995). This is a subtle yet crucial aspect of the technique. Directional control in a soft robot could be achieved by independently actuating the left and right fins or segments, allowing for precision turns and adjustments in the water. Similar to how a butterfly swimmer adjusts direction with slight body tweaks, a soft robot could have pressure sensors or feedback mechanisms that control the inflation levels of its actuators to alter swimming direction. Utilizing a feedback system can help ensure that the robot remains on course while performing complex swimming manoeuvres.

4.6 Summary

In summary, the soft robot demonstrated the ability to swim in a linear path. The optimal swimming performance for this linear motion was achieved at an actuation frequency of 1.33 Hz and a pump voltage of 11 V. The directional control feature was successfully validated, allowing the robot to change direction as needed. Finally, the linear swimming mode and directional control were integrated into a swimming algorithm, controlled via three push buttons, to manage left, right, and straight movement.

CHAPTER 5

CONCLUSIONS AND RECOMMENDATIONS

5.1 Conclusions

In conclusion, the objectives of this project were successfully achieved. The small swimming soft robot demonstrated the ability to swim on water surface and effectively control its yaw. The design of the soft robot was carefully developed after reviewing existing designs, followed by fabrication and performance testing. The robot's buoyancy and straight-line swimming capabilities were evaluated, after which optimal parameters for actuation were determined. Directional control was then validated to ensure manoeuvrability. Given the presence of water near electronic components, safety measures, such as isolating the control circuit with an insulator, were implemented to prevent any electrical hazards. Furthermore, this Final Year Project (FYP) was recognized in the FYP poster competition, earning a bronze award. Supporting documentation for this achievement can be found in Appendix B and Appendix C.

5.2 Recommendations for Future Work

Several challenges were encountered during the project, with recommendations provided for future improvements. One major issue arose from the fabrication process, which involved bonding three layers, and silicone tubes to form the soft actuator. The actuator tended to burst along the bonding edges. In this project, the issue was addressed by reinforcing the joints with additional Ecoflex. For future work, it is recommended to cure the soft actuator as a single unit. A possible approach could involve using solidified wax to form a mold for the pneumatic chambers, then pouring uncured Ecoflex into its own mold and inserting the wax structure into the center of the Ecoflex before curing, ensuring more robust and uniform chamber formation, on top of bonding the silicone tube together instead of afterward.

Additionally, there was significant wastage of Ecoflex during fabrication, as the precise quantity required was not known at the outset. Measuring and remeasuring Ecoflex proved inefficient, often leading to an excess being poured. To resolve this issue, it is suggested that the amount of Ecoflex needed be determined through software analysis, using a tool like the volume analysis function in SOLIDWORKS to calculate the required quantity more accurately. This would reduce material waste and streamline the fabrication process.

REFERENCES

- Arellano, R., Brown, P., Cappaert, J. and Nelson, R.C., 2006. Analysis of 50-m male and female butterfly swimmers at the 1992 Olympic Games. *Journal of Applied Biomechanics*, 12(2), pp.189-204.
- Ariati, R., Sales, F., Souza, A., Lima, R.A. & Ribeiro, J.J.P., 2021. Polydimethylsiloxane composites characterization and its applications: a review. *Polymer Testing*, 104, 106457.
- Baechle, D.M., Kothera, C.S., Lewis, J.A. & Vaia, R.A., 2013. Explosive actuators: fundamentals, energetic materials, and applications. *Advanced Materials*, 25(31), pp.5085-5108.
- Brown, A. & Smith, B., 2019. Soft robotics in marine applications: a review. *Marine Technology Society Journal*, 53(2), pp.15-28.
- Calisti, M., Cianchetti, M. & Arienti, A., 2018. Soft robotics technologies to address shortcomings in today's underwater manipulation and locomotion. *IEEE Robotics & Automation Magazine*, 25(2), pp.20-30.
- Chollet, D., Chabies, S. and Chatard, J.C., 2006. A new index of coordination for the crawl: Description and usefulness. *International Journal of Sports Medicine*, 27(1), pp.123-129.
- El-Atab, N., Mishra, R., Al-modaf, F., Joharji, L., Alsharif, A., Alamoudi, H., Diaz, M. & Qaiser, N., 2020. Soft actuators for soft robotic applications: a review. *Advanced Intelligent Systems*, 2, 2000128.
- Fan, J. et al., 2020. Swimming performance of the frog-inspired soft robot. *Soft Robotics*, 7(5), pp.615–626. doi:10.1089/soro.2019.0094.
- Gibson, I., Rosen, D.W. & Stucker, B., 2014. *Additive manufacturing technologies: 3D printing, rapid prototyping, and direct digital manufacturing*. Springer.
- Gorissen, B., Reynaerts, D., Konishi, S. & Yoshida, K., 2017. Miniature soft pneumatic actuators for robotic applications: a review. *Journal of Intelligent Material Systems and Structures*, 28(18), pp.2457-2474.
- Hu, W., Lum, G.Z., Mastrangeli, M. and Sitti, M., 2020. Small-scale soft-bodied robot with multimodal locomotion. *Nature*, 554(7698), pp.81-85.
- Ilievski, F., Mazzeo, A.D., Shepherd, R.F., Chen, X. & Whitesides, G.M., 2011. Soft robotics for chemists. *Angewandte Chemie International Edition*, 50(8), pp.1890-1895.

- Kim, J., Hanna, J.A., Byun, M., Santangelo, C.D. & Hayward, R.C., 2012. Designing responsive buckled surfaces by halftone gel lithography. *Science*, 335(6073), pp.1201-1205.
- Kim, J., Yuk, H., Zhao, R., Chester, S.A. & Zhao, X., 2018. Printing ferromagnetic domains for untethered fast-transforming soft materials. *Nature*, 558(7709), pp.274-279.
- Kim, J., Lee, S. & Park, H., 2020. Soft materials for biomimetic robotic systems. *Nature Robotics*, 4(2), pp.123-130.
- Kim, Y., Parada, G.A., Liu, S. and Zhao, X., 2021. Ferromagnetic soft continuum robots. *Science Robotics*, 4(33), eaax7329.
- Lee, H.R., Kim, C.C. & Sun, J.Y., 2018. Stretchable ionics—a promising candidate for upcoming wearable devices. *Journal of Materials Chemistry A*, 30, 1704403.
- Lendlein, A. & Langer, R., 2002. Biodegradable, elastic shape-memory polymers for potential biomedical applications. *Science*, 296(5573), pp.1673-1676.
- Li, M., Chen, R. and Sun, Z., 2020. Soft actuators in underwater robotics. *Robotics and Autonomous Systems*, 126, pp.45-54.
- Liu, Y., Zhang, H. & Wang, D., 2021. Electroactive polymer actuators for soft robotics. *Journal of Advanced Robotics*, 37(4), pp.456-470.
- Marchese, A.D., Katzschmann, R.K. and Rus, D., 2014. A recipe for soft fluidic elastomer robots. *Soft Robotics*, 2(1), pp.7-25.
- Martinez, R.V., Glavan, A.C., Keplinger, C., Oyetibo, A.I. & Whitesides, G.M., 2013. Soft actuators and robots that are resistant to mechanical damage. *Advanced Functional Materials*, 23(36), pp.4428-4436.
- Mosadegh, B., Polygerinos, P., Keplinger, C., Wennstedt, S., Shepherd, R.F., Gupta, U. et al., 2015. Pneumatic networks for soft robotics that actuate rapidly. *Advanced Functional Materials*, 24(15), pp.2163-2170.
- Nguyen, D.Q. & Ho, V.A., 2022. Anguilliform swimming performance of an eel-inspired soft robot. *Soft Robotics*, 9(3), pp.425-439. doi:10.1089/soro.2020.0093.
- Park, T., Kim, S. & Oh, J., 2022. Biomimetic robots for coral reef exploration. *Marine Technology Journal*, 29(1), pp.25-35.
- Pelrine, R., Kornbluh, R., Pei, Q. & Joseph, J., 2000. High-speed electrically actuated elastomers with strain greater than 100%. *Science*, 287(5454), pp.836-839.

Polygerinos, P., Wang, Z., Galloway, K.C., Wood, R.J. & Walsh, C.J., 2015. Soft robotic glove for combined assistance and at-home rehabilitation. *Robotics and Autonomous Systems*, 73, pp.135-143.

Rus, D. & Sitti, M., 2014. Soft robotics: a perspective—current trends and prospects for the future. *Soft Robotics*, 1(1), pp.5-11.

Sanders, R.H., Psycharakis, S.G. and McCabe, C., 1995. A review of technique analysis for improving stroke efficiency. *Journal of Sports Sciences*, 33(2), pp.457-469.

Shen, L., Zhao, F. & Xu, W., 2020. Locomotion strategies for underwater soft robots. *IEEE Transactions on Robotics*, 36(3), pp.317-326.

Smith, J.R. & Johnson, A.R., 2017. Design and fabrication of a piezoelectric microvacuum pump. *Journal of Microelectromechanical Systems*, 26(5), pp.1092-1097.

Smith, J. & Jones, K., 2018. Environmental impact of robotic interventions in marine ecosystems: a review. *Environmental Science and Technology*, 45(3), pp.289-301.

Song, S.-H. et al., 2016. Turtle mimetic soft robot with two swimming gaits. *Bioinspiration & Biomimetics*, 11(3), p.036010. doi:10.1088/1748-3190/11/3/036010.

Srivastava, N. & Singh, P., 2020. *Hands-on Internet of Things with Blynk: Build on the power of Blynk to configure smart IoT projects*. Packt Publishing Ltd.

Tondu, B. & Lopez, P.J., 2000. Modeling and control of McKibben artificial muscle robot actuators. *IEEE Control Systems Magazine*, 20, pp.15-38.

Toussaint, H.M., Roos, P.E. and Kolmogorov, S., 2006. The determination of drag in front crawl swimming. *Journal of Biomechanics*, 41(2), pp.270-276.

Trivedi, D., Rahn, C.D., Kier, W.M. & Walker, I.D., 2008. Soft robotics: biological inspiration, state of the art, and future research. *Applied Bionics and Biomechanics*, 5(3), pp.99-117.

Uchino, K., 2008. *Ferroelectric devices*. CRC Press.

Veiga, S., Cala, A., Mallo, J. and Navarro, E., 2014. A new procedure for race analysis in swimming based on individual distance measurements. *Journal of Sports Sciences*, 32(2), pp.159-165.

Wang, D., Li, X. & Zhang, M., 2019. Pneumatic actuation systems in soft robotics. *Advanced Materials Robotics*, 25(6), pp.1010-1022.

Wang, J., Tham, D., Wei, Z. & Liu, A.Q., 2018. A high-throughput microfluidic cell sorting system based on integrated micro-solenoid valves. *Lab on a Chip*, 18(16), pp.2381-2390.

Wang, L., 2018. Energy-efficient designs for soft robotics. *International Journal of Robotics Research*, 37(9), pp.1010-1023.

Wang, N.F., Chaoyu, C., Guo, H., Chen, B. & Zhang, X., 2017. Advances in dielectric elastomer actuation technology. *Science China Technological Sciences*, 61, DOI: 10.1007/s11431-017-9140-0.

White, T.J., Broer, D.J. & Remsing, R.C., 2015. Thermal-mechanical properties of liquid crystal elastomers. *Journal of Polymer Science Part B: Polymer Physics*, 53(24), pp.1721-1730.

Wurth, S., Capogrosso, M., Raspopovic, S., Gandar, J., Federici, G., Kinany, N. et al., 2017. Long-term usability and bio-integration of polyimide-based intra-neural stimulating electrodes. *Biomaterials*, 122, pp.114-129.

Yang, T., Wang, P. and Zhao, X., 2019. Bio-inspired propulsion mechanisms for underwater robots. *Journal of Soft Robotics*, 6(3), pp.256-267.

Yin, C. et al., 2021. Visible light-driven jellyfish-like miniature swimming soft robot. *ACS Applied Materials & Interfaces*, 13(39), pp.47147-47154. doi:10.1021/acsami.1c13975.

Yuk, H., Lu, B. & Zhao, X., 2019. Hydrogel bioelectronics. *Chemical Society Reviews*, 48, pp.1642-1667.

Zhang, Y. and Liu, Q., 2021. High-performance actuators for soft robots. *IEEE Transactions on Robotics*, 37(7), pp.1120-1131.

Zhu, X., Li, W. & Chen, M., 2018. Butterfly-inspired flapping robots for underwater propulsion. *Robotics and Autonomous Systems*, 101(5), pp.135-142.

APPENDICES

Appendix A: Coding for Swimming Algorithm

```
1 // Pin assignments for relays
2 const int relayLeftUpper = 2; // Relay 1: Left Upper Channel
3 const int relayLeftLower = 3; // Relay 2: Left Lower Channel
4 const int relayRightUpper = 4; // Relay 3: Right Upper Channel
5 const int relayRightLower = 5; // Relay 4: Right Lower Channel
6
7 // Pin assignments for buttons
8 const int buttonSwimLeft = 8; // Button 1
9 const int buttonSwimRight = 9; // Button 2
10 const int buttonSwimStraight = 10; // Button 3
11
12 // Variable to store the current mode
13 int currentMode = 0;
14
15 void setup() {
16     // Initialize relay pins as outputs
17     pinMode(relayLeftUpper, OUTPUT);
18     pinMode(relayLeftLower, OUTPUT);
19     pinMode(relayRightUpper, OUTPUT);
20     pinMode(relayRightLower, OUTPUT);
21
22     // Initialize button pins as inputs
23     pinMode(buttonSwimLeft, INPUT_PULLUP);
24     pinMode(buttonSwimRight, INPUT_PULLUP);
25     pinMode(buttonSwimStraight, INPUT_PULLUP);
26
27     // Ensure all relays are off initially (assuming active-low relays)
28     digitalWrite(relayLeftUpper, HIGH);
29     digitalWrite(relayLeftLower, HIGH);
30     digitalWrite(relayRightUpper, HIGH);
31     digitalWrite(relayRightLower, HIGH);
32 }
33
```

```
void loop() {  
  // Check which button is pressed and set the current mode accordingly  
  if (digitalRead(buttonSwimLeft) == LOW) {  
    currentMode = 1; // Swim Left mode  
  } else if (digitalRead(buttonSwimRight) == LOW) {  
    currentMode = 2; // Swim Right mode  
  } else if (digitalRead(buttonSwimStraight) == LOW) {  
    currentMode = 3; // Swim Straight mode  
  }  
  
  // Execute the appropriate mode based on the current mode value  
  switch (currentMode) {  
    case 1:  
      swimLeft();  
      break;  
    case 2:  
      swimRight();  
      break;  
    case 3:  
      swimStraight();  
      break;  
    default:  
      // No mode selected, keep relays off  
      digitalWrite(relayLeftUpper, HIGH);  
      digitalWrite(relayLeftLower, HIGH);  
      digitalWrite(relayRightUpper, HIGH);  
      digitalWrite(relayRightLower, HIGH);  
      break;  
  }  
}
```

```
// Function for Swim Left mode (alternate relays 3 and 4)
void swimLeft() {
    digitalWrite(relayRightUpper, LOW); // Activate relay 3 (Right Upper)
    digitalWrite(relayRightLower, HIGH); // Deactivate relay 4 (Right Lower)
    delay(500);

    digitalWrite(relayRightUpper, HIGH); // Deactivate relay 3 (Right Upper)
    digitalWrite(relayRightLower, LOW); // Activate relay 4 (Right Lower)
    delay(500);
}

// Function for Swim Right mode (alternate relays 1 and 2)
void swimRight() {
    digitalWrite(relayLeftUpper, LOW); // Activate relay 1 (Left Upper)
    digitalWrite(relayLeftLower, HIGH); // Deactivate relay 2 (Left Lower)
    delay(500);

    digitalWrite(relayLeftUpper, HIGH); // Deactivate relay 1 (Left Upper)
    digitalWrite(relayLeftLower, LOW); // Activate relay 2 (Left Lower)
    delay(500);
}

// Function for Swim Straight mode (alternate relays 1 & 3 and 2 & 4)
void swimStraight() {
    digitalWrite(relayLeftUpper, LOW); // Activate relay 1 (Left Upper)
    digitalWrite(relayRightUpper, LOW); // Activate relay 3 (Right Upper)
    digitalWrite(relayLeftLower, HIGH); // Deactivate relay 2 (Left Lower)
    digitalWrite(relayRightLower, HIGH); // Deactivate relay 4 (Right Lower)
    delay(500);

    digitalWrite(relayLeftUpper, HIGH); // Deactivate relay 1 (Left Upper)
    digitalWrite(relayRightUpper, HIGH); // Deactivate relay 3 (Right Upper)

    digitalWrite(relayLeftLower, LOW); // Activate relay 2 (Left Lower)
    digitalWrite(relayRightLower, LOW); // Activate relay 4 (Right Lower)
    delay(500);
}
```

Appendix B: Supporting attachment for FYP Competition Shortlisting

UTAR UNIVERSITI TUNKU ABDUL RAHMAN
Lee Kong Chian Faculty of Engineering and Science **LKC**

DESIGN OF A SMALL SWIMMING SOFT ROBOT FOR UNDERWATER APPLICATION

Prepared by Chavez Chen Zhen Ming under supervision of Dr. Low Jan Hahn

ABSTRACT
An approach to the traditional rigid robots find the role of observing biome to humans and other organisms. Flexible and adaptable soft robots can perform tasks adaptability. This study explores the fabrication mechanism of artificial soft robot to be applied for a small swimming soft robot, utilizing elastic and deformable materials like Ecoflex, PVC sheet, and plastic film, a swimming soft robot that can operate in water to detect and its swimming performance is analyzed. A directional control feature is also added in the second prototype to improve its maneuverability. The research outcome will also be used for testing on the swimming efficiency of robot and the practical applications in marine and underwater exploration, and water quality monitoring.

OBJECTIVES

- To review soft robots in terms of design, materials, and locomotion algorithm.
- To design a soft robot using soft material.
- To develop an algorithm of robot swimming locomotion using deformable anisotropic mechanism.

METHODOLOGY

Simulation
The deformation of soft actuator made of Ecoflex under air pressure is simulated in COMSOL Multiphysics software.

Creating Mold
Molds used for casting Ecoflex were designed in Solidworks and 3D printed.

Preparation of Ecoflex
Ecoflex 001 was used as the material. Part A and Part B are mixed and stirred for 10 minutes.

Fabrication of Prototype
Molds injection were prepared for the casting Ecoflex. The casting Ecoflex was done in the mold. The mold was filled with Ecoflex and left for 24 hours to cure. The Ecoflex was removed from the mold and the soft robot was fabricated.

Assembling Parts
The soft robot was assembled with the prepared parts. The soft robot was tested in water to see its swimming performance.

Electrical and Pneumatic Circuit
The soft robot was connected to a microcontroller and a pump. The microcontroller was used to control the pump and the soft robot.

Swimming Performance Evaluation
The swimming performance of the soft robot was evaluated by measuring the distance it can swim in a given time.

Directional Control Validation
The soft robot was tested to see if it can swim in a specific direction.

RESULTS

Simulation
Figure 1: Computational fluid dynamics (CFD) simulation of soft actuator motion patterns at high pressure. Figure 2: Computational fluid dynamics (CFD) simulation of soft actuator motion patterns at low pressure.

Characterisation
Figure 3: Graph of pressure (kPa) vs. time (s) for high pressure. Figure 4: Graph of pressure (kPa) vs. time (s) for low pressure.

Control Signal
Figure 5: Graph of control signal vs. time (s) for high pressure. Figure 6: Graph of control signal vs. time (s) for low pressure.

Swimming Performance
Figure 7: Graph of distance (cm) vs. time (s) for high pressure. Figure 8: Graph of distance (cm) vs. time (s) for low pressure.

Directional Control
Figure 9: Graph of distance (cm) vs. time (s) for high pressure. Figure 10: Graph of distance (cm) vs. time (s) for low pressure.

Video GIF
Figure 11: Video GIF of the soft robot swimming in water.

APPLICATION

Search and Rescue
Application in high pressure for being flexible.

Water Quality Monitoring
Application in high pressure for being flexible.

CONCLUSION
The research outcome has shown that the soft robot can swim in water and change its direction. The robot has potential applications in marine and underwater exploration, and water quality monitoring.

UTAR LKC FES Page
9月6日 16:24

DMBE \ T3-01 : Design of a small swimming soft robot for underwater applications -- Like this poster? Vote for it at <https://forms.gle/EYid9wtCx1aYofpHA>

云圣颖、Stephanie Kok和其他4位用户 1

写评论...

Appendix C: Supporting attachment for FYP Competition Bronze Award



Appendix D: Open Access to Image Rights

SPRINGER NATURE LICENSE TERMS AND CONDITIONS

Sep 18, 2024

This Agreement between Chavez ("You") and Springer Nature ("Springer Nature") consists of your license details and the terms and conditions provided by Springer Nature and Copyright Clearance Center.

License Number	5871970687305
License date	Sep 18, 2024
Licensed Content Publisher	Springer Nature
Licensed Content Publication	Nature
Licensed Content Title	Shape memory polymer with programmable recovery onset
Licensed Content Author	Chujun Ni et al
Licensed Content Date	Sep 13, 2023
Type of Use	Thesis/Dissertation
Requestor type	academic/university or research institute

Figure D- 1: Shape memory polymer with programmable recovery onset.

RightsLink

You have been directed to this webpage as a result of the type of license signed between the author and the American Chemical Society that provides users with some different terms of use.

Open Access licenses

If the article is open access and uses a Creative Commons public use license, e.g., CC-BY or CC-BY-NC-ND, a human readable summary of its permitted uses can be found by clicking on the "View License Deed" at <https://creativecommons.org/licenses/>. For permission to use the CC-licensed work beyond what is allowed by the license, please contact ACS at support@services.acs.org with your request.

If the article is open access and does not use a Creative Commons license, it is subject to the terms of an ACS public use license. For rights and permissions questions about ACS public use licenses, contact support@services.acs.org with your request, including the following information:

- A link to the ACS article from which you wish to reuse content
- The portion of content you wish to reuse (e.g., number of figures, entire article for thesis)
- A description of where the content will be reused (e.g., name of journal, book title, thesis)

Figure D- 2: Second-Generation Soft Actuators Driven by NIR Light Based on Croconaine Dye-Doped Vitrimers.



Cyclic hydraulic actuation for soft robotic devices
 Conference Proceedings: 2016 IEEE/RSJ International Conference on Intelligent Robots and Systems (IROS)
 Author: Robert K Katschmann
 Publisher: IEEE
 Date: October 2016
 Copyright © 2016, IEEE

Thesis / Dissertation Reuse

The IEEE does not require individuals working on a thesis to obtain a formal reuse license, however, you may print out this statement to be used as a permission grant:

Requirements to be followed when using any portion (e.g., figure, graph, table, or textual material) of an IEEE copyrighted paper in a thesis:

- 1) In the case of textual material (e.g., using short quotes or referring to the work within these papers) users must give full credit to the original source (author, paper, publication) followed by the IEEE copyright line © 2011 IEEE.
- 2) In the case of illustrations or tabular material, we require that the copyright line © [year of original publication] IEEE appear prominently with each reprinted figure and/or table.
- 3) If a substantial portion of the original paper is to be used, and if you are not the senior author, also obtain the senior author's approval.

Requirements to be followed when using an entire IEEE copyrighted paper in a thesis:

- 1) The following IEEE copyright/ credit notice should be placed prominently in the references: © [year of original publication] IEEE. Reprinted, with permission, from [author names, paper title, IEEE publication title, and month/year of publication]
- 2) Only the accepted version of an IEEE copyrighted paper can be used when posting the paper or your thesis on-line.
- 3) In placing the thesis on the author's university website, please display the following message in a prominent place on the website: In reference to IEEE copyrighted material which is used with permission in this thesis, the IEEE does not endorse any of [university/educational entity's name goes here]'s products or services. Internal or personal use of this material is permitted. If interested in reprinting/republishing IEEE copyrighted material for advertising or promotional purposes or for creating new collective works for resale or redistribution, please go to http://www.ieee.org/publications_standards/publications/rights/rights_link.html to learn how to obtain a License from RightsLink.

If applicable, University Microfilms and/or ProQuest Library, or the Archives of Canada may supply single copies of the dissertation.

BACK

CLOSE WINDOW

Figure D- 3: Cyclic hydraulic actuation for soft robotic devices.

JOHN WILEY AND SONS LICENSE
 TERMS AND CONDITIONS

Sep 18, 2024

This Agreement between Chavez ("You") and John Wiley and Sons ("John Wiley and Sons") consists of your license details and the terms and conditions provided by John Wiley and Sons and Copyright Clearance Center.

License Number	5871970141588
License date	Sep 18, 2024
Licensed Content Publisher	John Wiley and Sons
Licensed Content Publication	Advanced Materials
Licensed Content Title	Robotic Tentacles with Three-Dimensional Mobility Based on Flexible Elastomers
Licensed Content Author	George M. Whitesides, Zhigang Suo, Rui M. D. Nunes, et al
Licensed Content Date	Sep 7, 2012
Licensed Content Volume	25

Print This Page

Figure D- 4: Robotic Tentacles with Three - Dimensional Mobility Based on Flexible Elastomers

MARY ANN LIEBERT, INC. LICENSE
TERMS AND CONDITIONS

Sep 18, 2024

This Agreement between Chavez ("You") and Mary Ann Liebert, Inc. ("Mary Ann Liebert, Inc.") consists of your license details and the terms and conditions provided by Mary Ann Liebert, Inc. and Copyright Clearance Center.

License Number	5871960927238
License date	Sep 18, 2024
Licensed Content Publisher	Mary Ann Liebert, Inc.
Licensed Content Publication	Soft Robotics
Licensed Content Title	Swimming Performance of the Frog-Inspired Soft Robot
Licensed Content Author	Jizhuang Fan, Shuqi Wang, Qingguo Yu, et al
Licensed Content Date	Oct 1, 2020
Licensed Content Volume	7
Licensed Content Issue	5
Type of Use	Dissertation/Thesis

[Print This Page](#)

Figure D- 5: Swimming Performance of the Frog-Inspired Soft Robot.

SPRINGER NATURE LICENSE
TERMS AND CONDITIONS

Sep 18, 2024

This Agreement between Chavez ("You") and Springer Nature ("Springer Nature") consists of your license details and the terms and conditions provided by Springer Nature and Copyright Clearance Center.

License Number	5871960629685
License date	Sep 18, 2024
Licensed Content Publisher	Springer Nature
Licensed Content Publication	Applied Physics A: Materials Science & Processing
Licensed Content Title	Flexible and stretchable electrodes for dielectric elastomer actuators
Licensed Content Author	Samuel Rosset et al
Licensed Content Date	Nov 7, 2012
Type of Use	Thesis/Dissertation

[Print This Page](#)

Figure D- 6: Flexible and stretchable electrodes for dielectric elastomer actuators

MARY ANN LIEBERT, INC. LICENSE
TERMS AND CONDITIONS

Sep 18, 2024

This Agreement between Chavez ("You") and Mary Ann Liebert, Inc. ("Mary Ann Liebert, Inc.") consists of your license details and the terms and conditions provided by Mary Ann Liebert, Inc. and Copyright Clearance Center.

License Number	5871961161630
License date	Sep 18, 2024
Licensed Content Publisher	Mary Ann Liebert, Inc.
Licensed Content Publication	Soft Robotics
Licensed Content Title	Anguilliform Swimming Performance of an Eel-Inspired Soft Robot
Licensed Content Author	Dinh Quang Nguyen, Van Anh Ho
Licensed Content Date	Jun 1, 2022
Licensed Content Volume	9
Licensed Content Issue	3

[Print This Page](#)

Figure D- 7: Anguilliform Swimming Performance of an Eel-Inspired Soft Robot

SPRINGER NATURE LICENSE
TERMS AND CONDITIONS

Sep 18, 2024

This Agreement between Chavez ("You") and Springer Nature ("Springer Nature") consists of your license details and the terms and conditions provided by Springer Nature and Copyright Clearance Center.

License Number	5871960014509
License date	Sep 18, 2024
Licensed Content Publisher	Springer Nature
Licensed Content Publication	Science China Technological Sciences
Licensed Content Title	Advances in dielectric elastomer actuation technology
Licensed Content Author	NianFeng Wang et al
Licensed Content Date	Nov 21, 2017
Type of Use	Thesis/Dissertation
Requestor type	academic/university or research institute
Format	electronic

[Print This Page](#)

Figure D- 8: Advances in dielectric elastomer actuation technology